Thermal behaviour, structure and dynamics of low-temperature water confined in mesoporous materials

T. Yamaguchi

Department of Chemistry, Fukuoka University
Advanced Materials Institute, Fukuoka University

Water at Interfaces, des Houches, 15–26 April 2013

Outline

- Introduction *Why is confined water important?*
- Water in MCM-41 *hydrophilic surface*
- Water in periodic mesoporous organosilica *hybrid (hydrophilic and hydrophobic) surface*
- Conclusions and Perspectives

Introduction: water in confinement and at interfaces plays an vital role in various fields

Water on/in proteins for food conservation, unfrozen water, and function of proteins

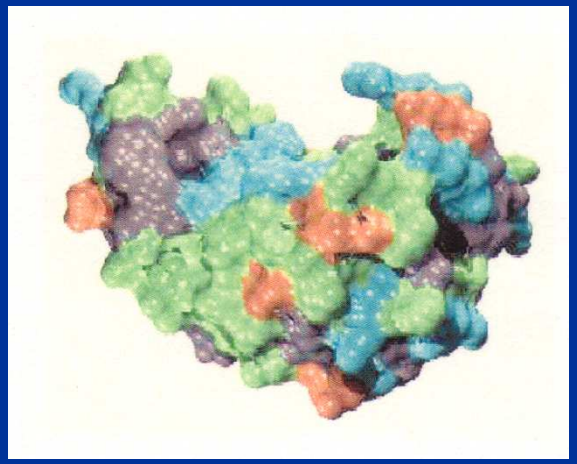

Tobias (2003)

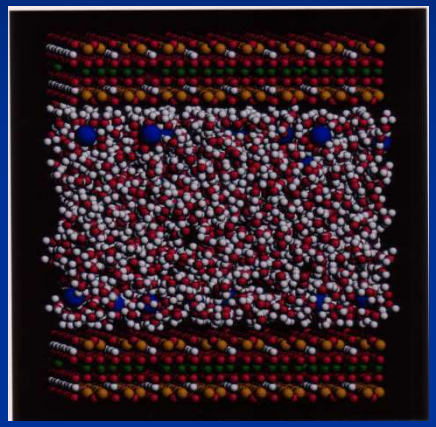

Skipper (1991)

Water in soils and clays for sedimentation and transfer of environmentally hazardous materials

Catalysts for chemical synthesis

Gel chromatography for separation of functional materials

Fuel cells, electrical double layers

Nano technology for one-dimensional materials, such as nanowire and nanotube

Puzzles of *bulk* liquid water from H.E. Stanley

- Volume fluctuations

  The compressibility of water is larger than that of normal liquids, and decreases with lowering temperature, but below 46 °C starts to increase.

- Entropy fluctuations

  The specific heat of water is larger than that of normal liquids, decrease when cooled, but starts to increase below about 35 °C.

- **Anomalous increase in thermodynamic quantities on approaching**

  a temperature of T_s = 228 K (Speedy & Angell).

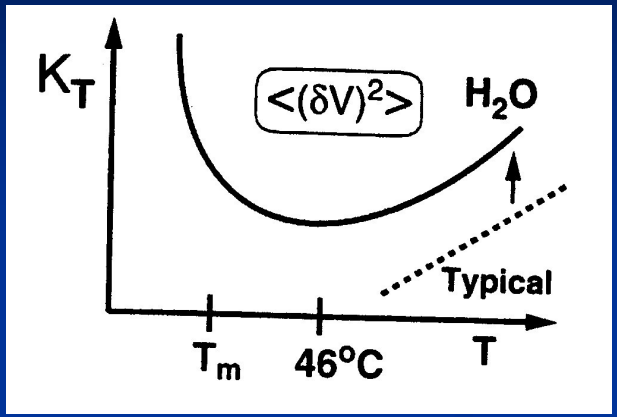

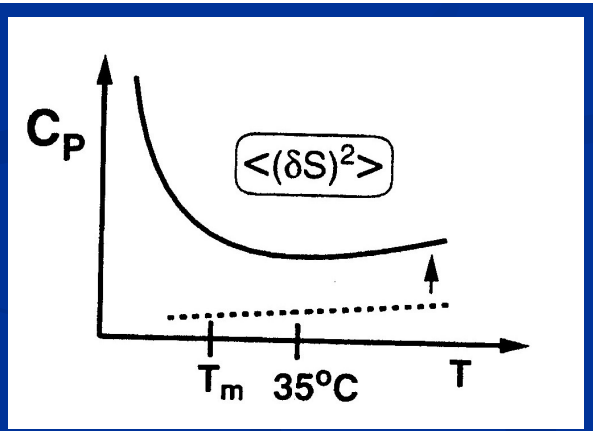

Various phases of *bulk* liquid water

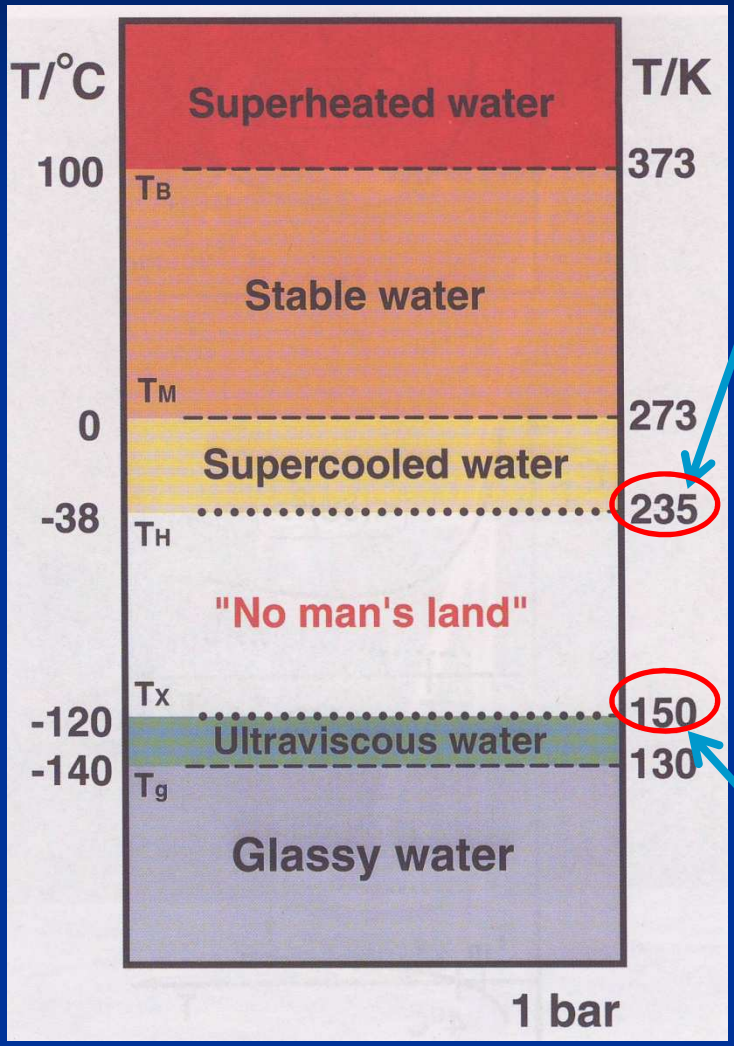

On Cooling supercooled water spontaneously freezes below T_H = 235 K (Homogeneous Nucleation Temperature)

No experiments except for simulations have been made to explore the properties of liquid water between 150 and 235 K. "No man's land" which covers T_s = 228 K

On heating, glassy water and ultraviscous water crystallise above T_X = 150 K.

From Stanley, in Hydration processes in Biology, Les Houches 1998, edited by M.C. Bellissent-Funel, Nato Science Series – Series A, vol 305, IOS Press (1999).

Hypothetical state diagram of *bulk* liquid water from a viewpoint of water polyamorphism

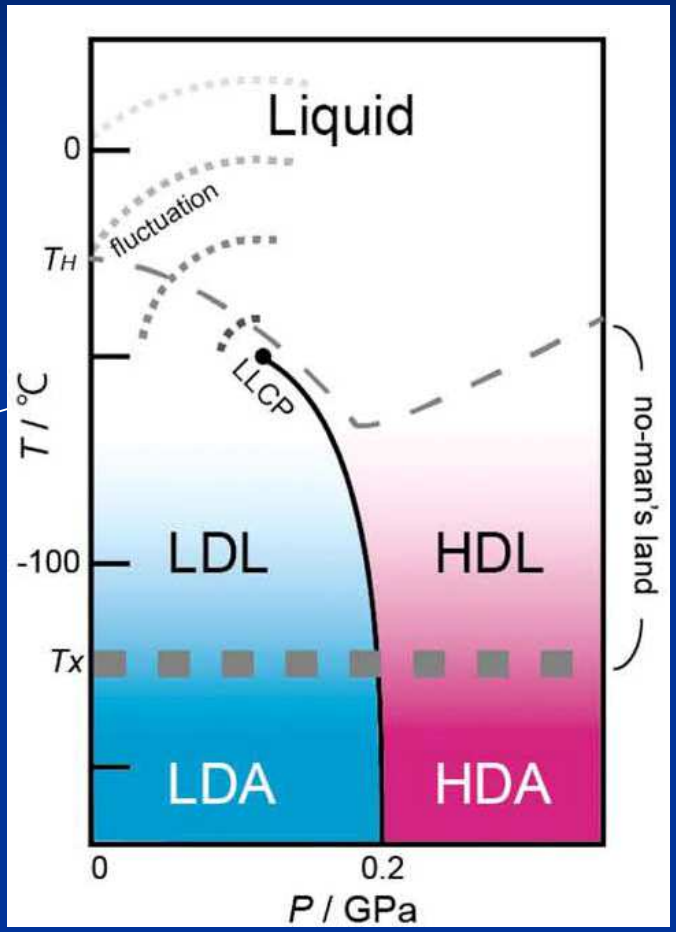

Taken from Suzuki (2013)

Two liquid water, low-density water (LDL) and high-density water (HDL) in a hypothetical supercooled region. A liquid-liquid critical point (LLCP) relating to two liquid water is postulated. When the LDL and HDL were cooled, they would change to LDA and HDA, respectively.

Photos of high-density amorphous ice (HDA) and low-density amorphous ice (LDA) at 1 bar

(Mishima & Stanley)

Confined water – connection to bulk water (?)

MCM-41 (Mobil Crystalline Materials) Highly controlled cylindrical channels

TEM

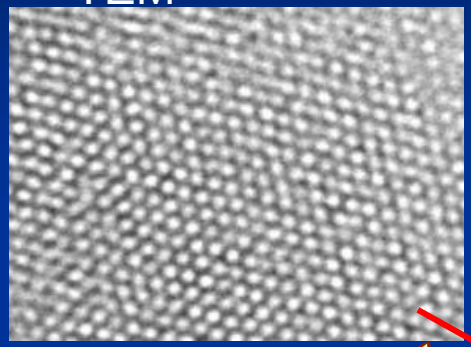

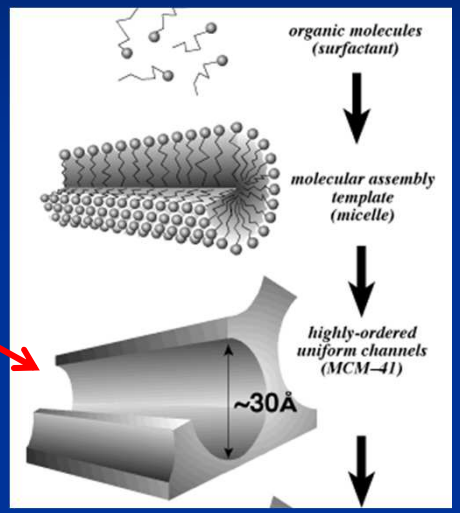

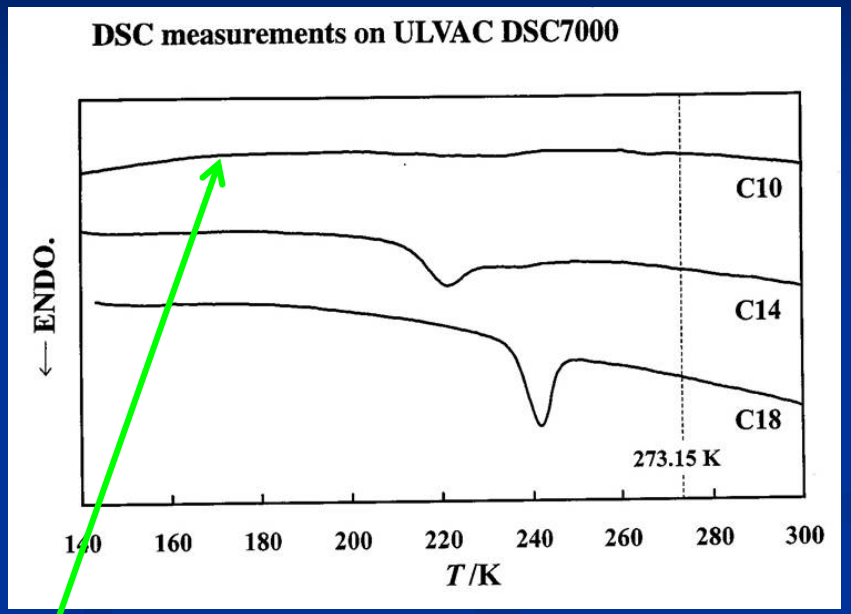

C10 (pore size 21 Å)

C14 (28 Å)

C18 (37 Å)

C_n; n = the number of C atoms in the alkyl group of surfactant

Mori, et al. Langmuir, 18 (2002) 1595.

In MCM-41 C10 water appears to be unfrozen down to 140 K which covers the no man's land T_s = 228 K.

Confined Water: model system to probe the structure and dynamics of water in the "No man's land"

Mesoporous silica: MCM-41, SBA-15, SBA-16

MCM-41

Beck, et al. JACS, 114 (1992) 10834

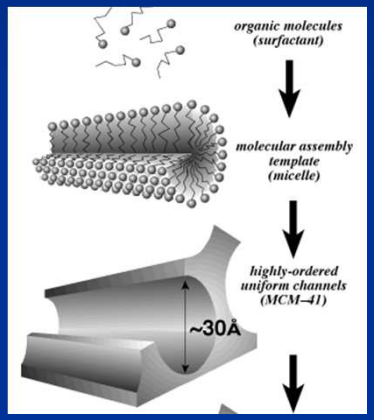

Cross sectional drawings

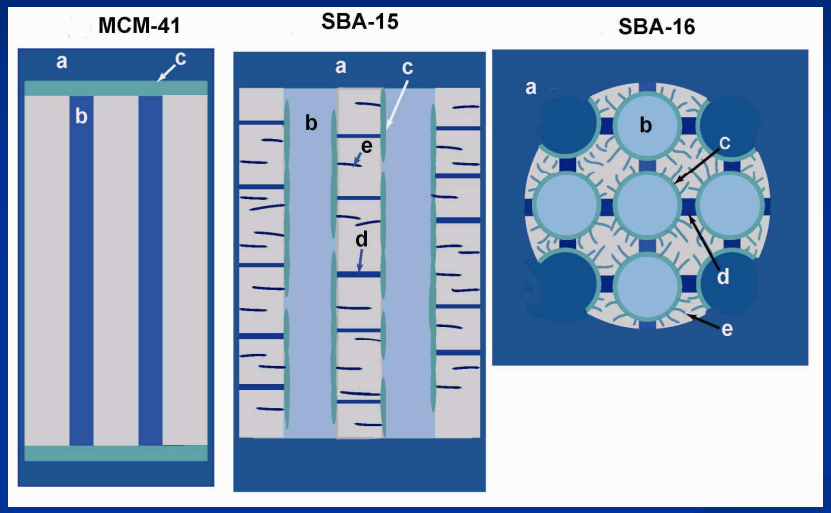

SBA-16

By Yang and Li (2010)

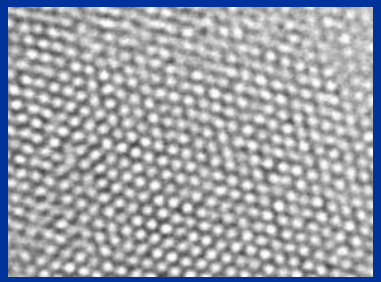

Highly controlled cylindrical channels

C10 (20 Å)

C14 (28 Å)

C n = number of C

SBA-15

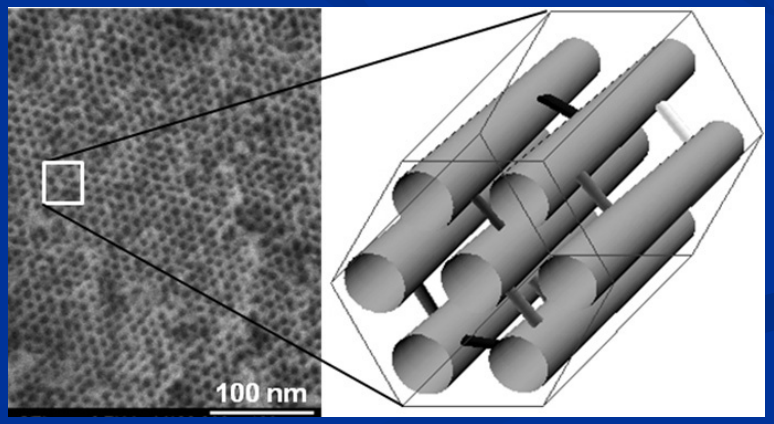

By Kleitz

How do the thermal behavior, structure, and dynamics of chemisorbed and physisorbed confined water change in confinement, compared with bulk?

Two effects: Confinement and interactions with walls

Physisorbed
water
Interfacial
Central part

Chemisorbed
water on the
wall surface

Silanol Si-OH
groups
I.P.=~4 (acidic)

Silica substrate

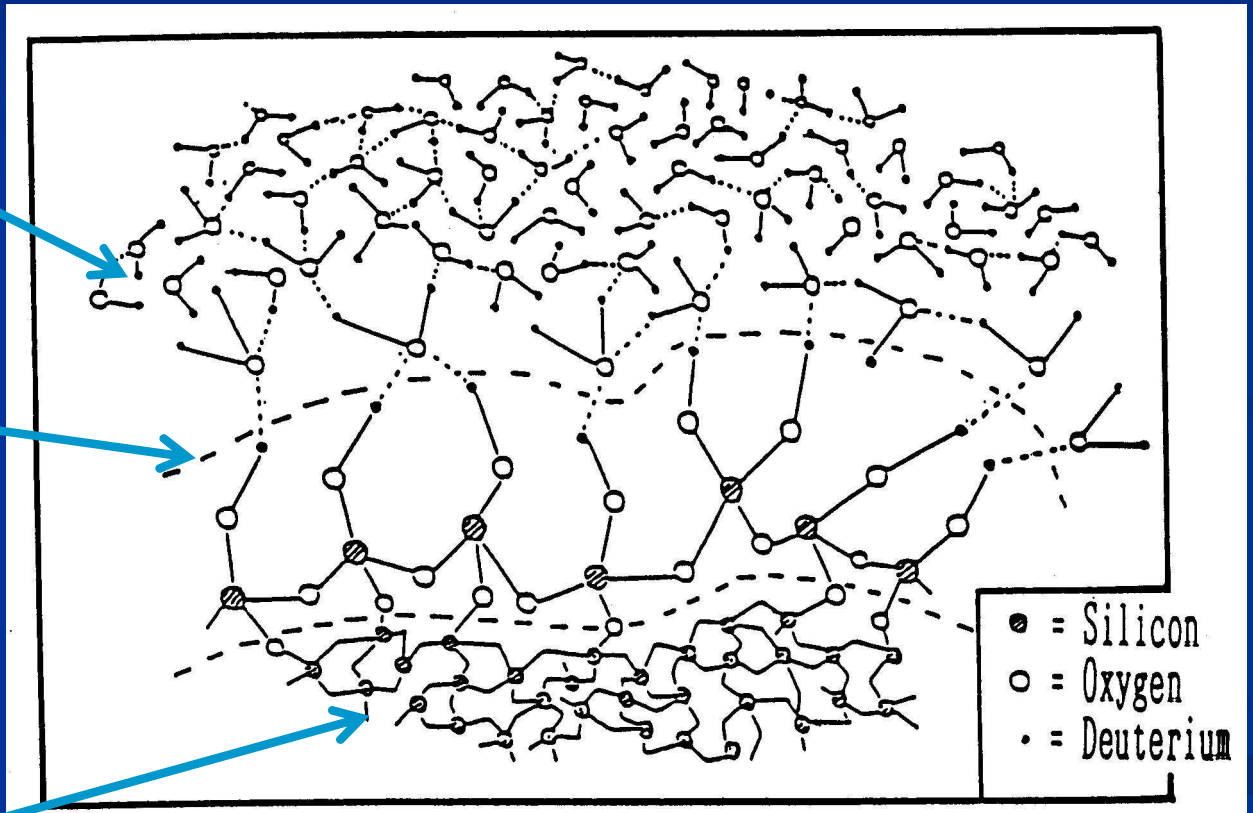

Model of confined water

J. C. Dore (1970)

Outline

- Introduction *Why is confined water important?*
- Water in MCM-41
- Water in periodic mesoporous organosilica
- Conclusions and Perspectives

Mesoporous materials MCM-41 to provide well characterized confinement

Independent cylindrical channels

Uniform pore size

Large surface area e.g. 1096 m^2/g for C10 (2.1 nm in diameter)

Hydrophilic surface –Si-OH
Note: ~3 OHs per 1 nm^2 !

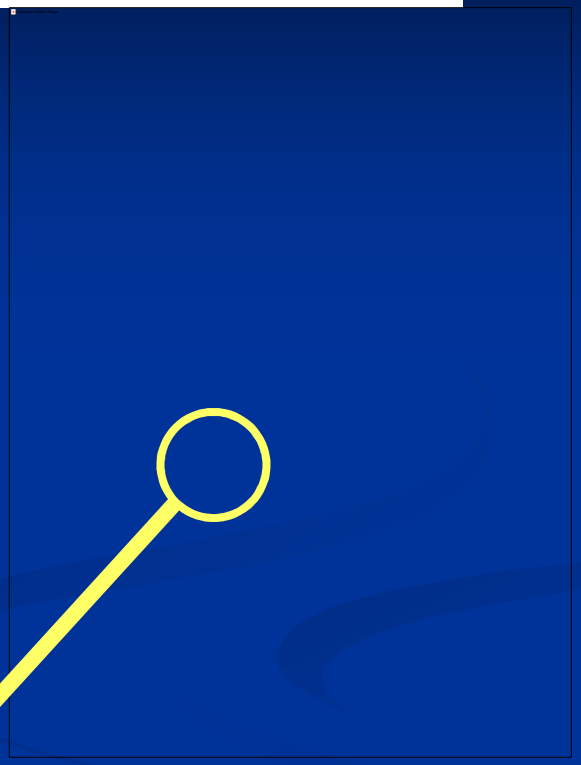

TEM of MCM-41

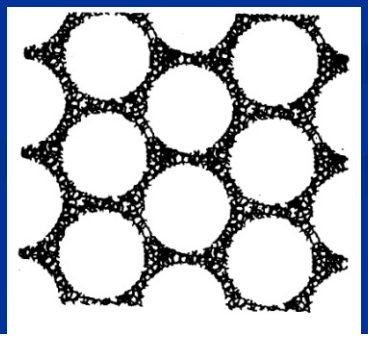

Adsorption (○) - desorption (●) isotherms of water on MCM-41 C10 at 298 K (Type V, IUPAC)

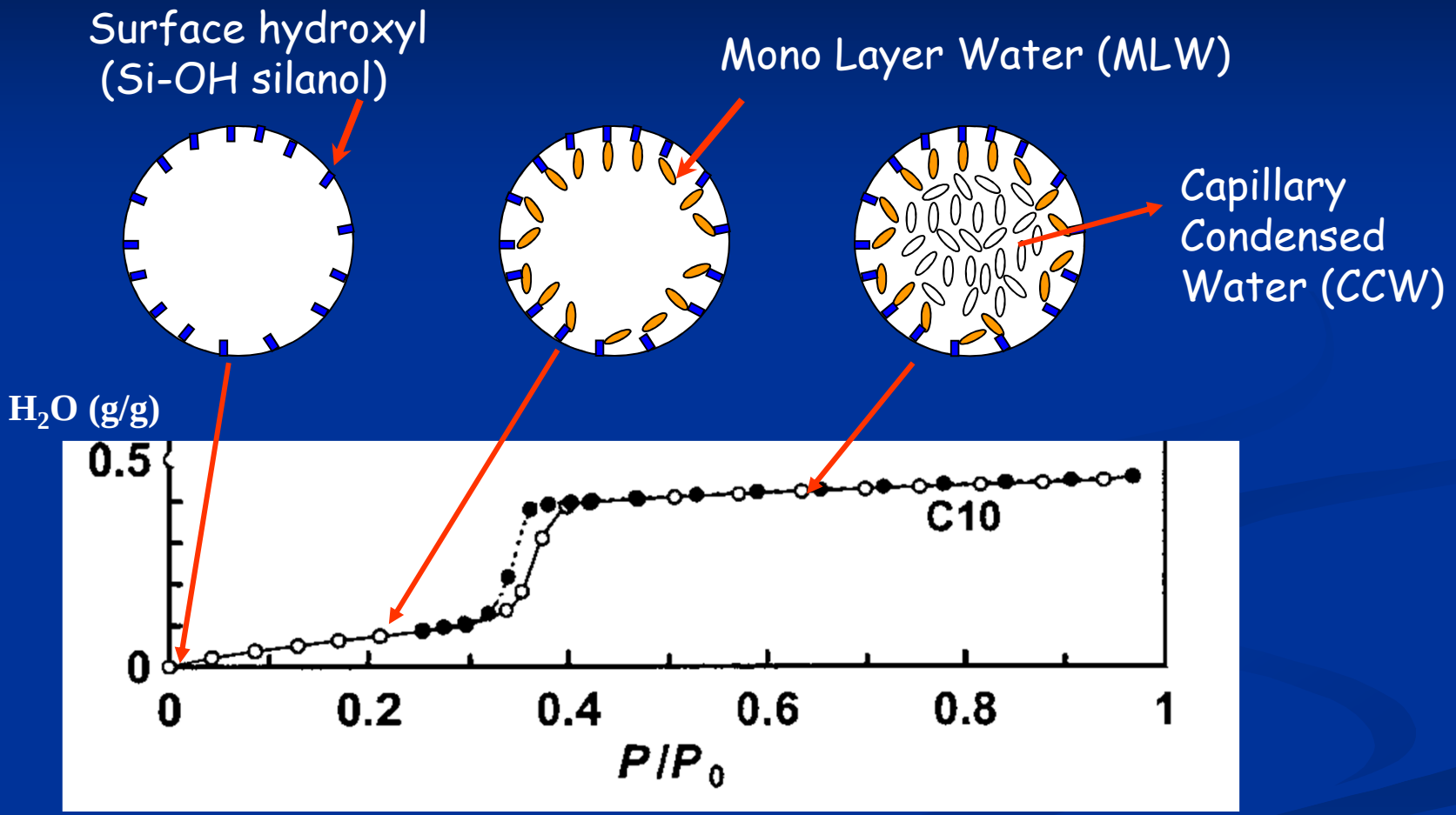

MLW and CCW states are easily prepared by adjusting the vapor pressure of water

Classification of adsorption/desorption by IUPAC (International Union of Pure and Applied Chemistry)

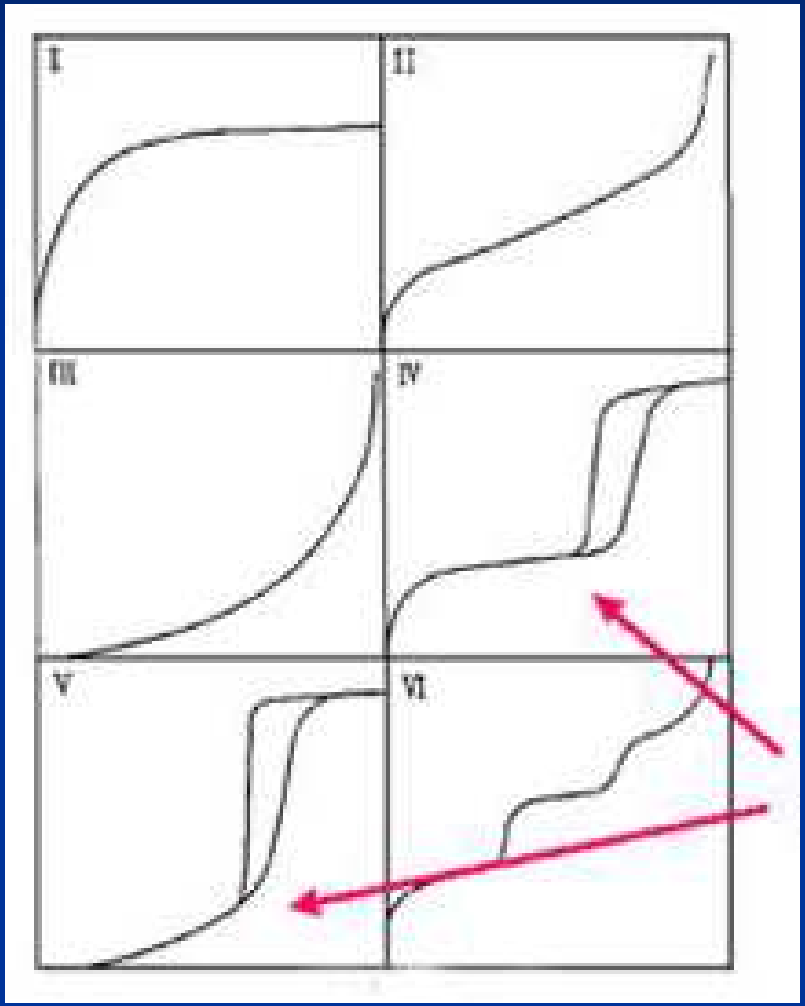

Type I : Micro pores (< 20 Å)

Type II and III: No mesopores or macro pores (> 500 Å)

Type IV and V: Meso pores (20 ~ 500 Å)

Type VI: Stepwise adsorption onto flat surface without pores

Hysteresis

Recent topics on water confined in MCM-41

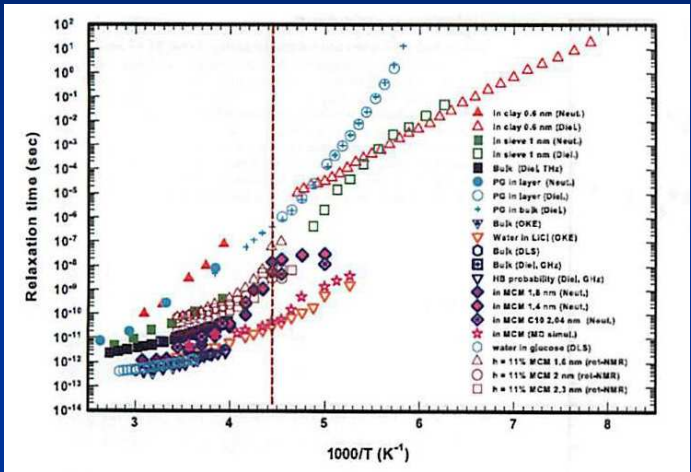

Dynamical crossover Fragile to Strong Liquid transition HDL-LDL transformation

Mallamace, et al. J. Phys.: Condens. Matter 24, 064103 (2012).

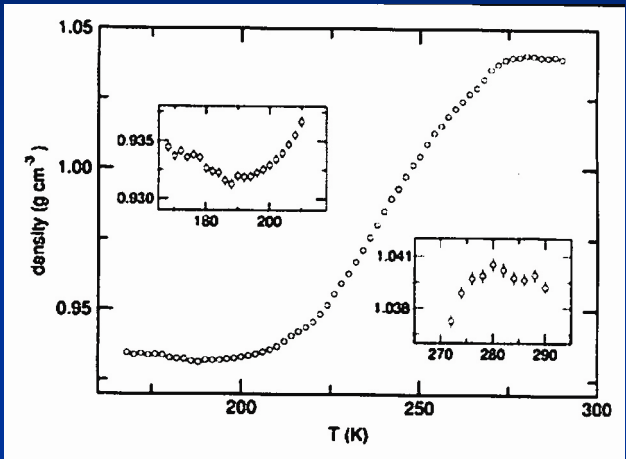

Minimum density occurs when water uniformly filled in pores,

Kamitakahara, et al. J. Phys.: Condens. Matter 24, 064106 (2012).

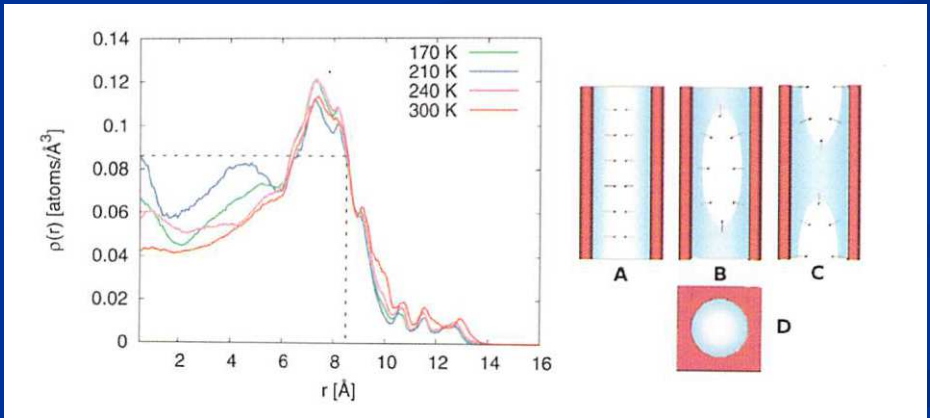

Distribution of water in the pores is not uniform.

Mancinelli, et al. J. Phys. Chem. Lett. 1, 1277 (2010).

Thermodynamic Properties of water confined in MCM-41

Kittaka, Takahara, Matsumoto, Wada, Satoh, T.Y. submitted

Heat capacity, Cp,

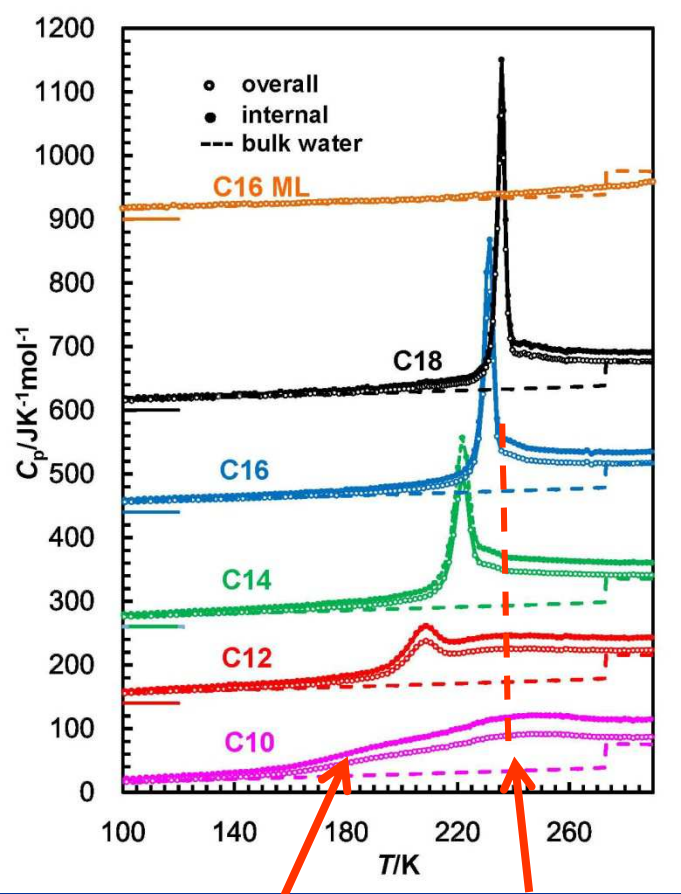

DSC (2 K/min)

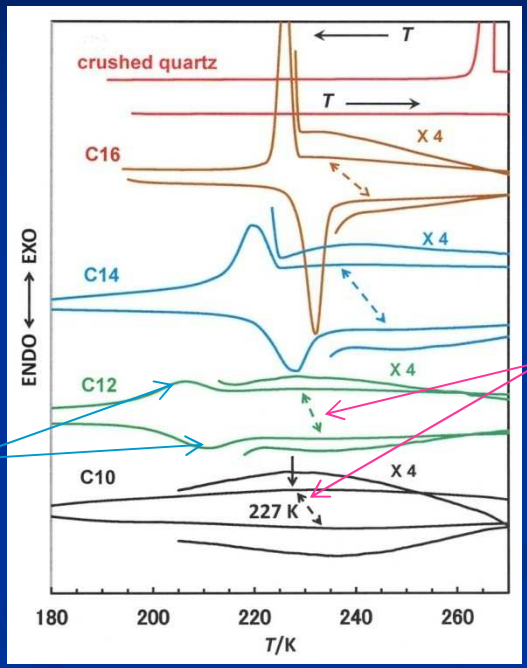

Freezing-melting

HDL-L DL transition

Gibbs-Thomson relation

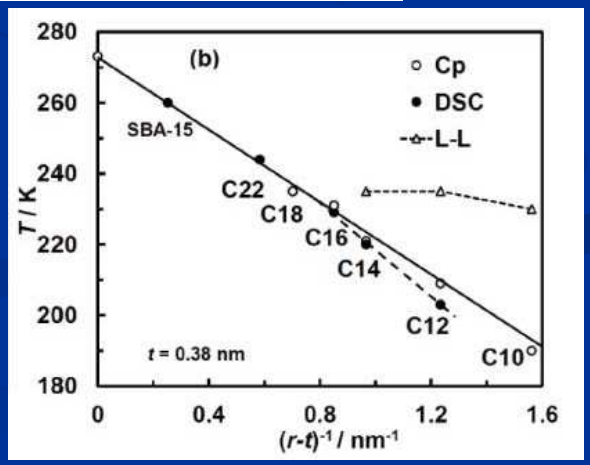

Glassy water / Ice melting at ~190 K

HDL-LDL transition at 230~240 K (close to HNT)

Gibbs-Thomson relationship : melting temperature vs. inverse effective pore radius

Kittaka, Ueda, Fujisaki, Iiyama, TY, PCCP, 13(2011)17222.

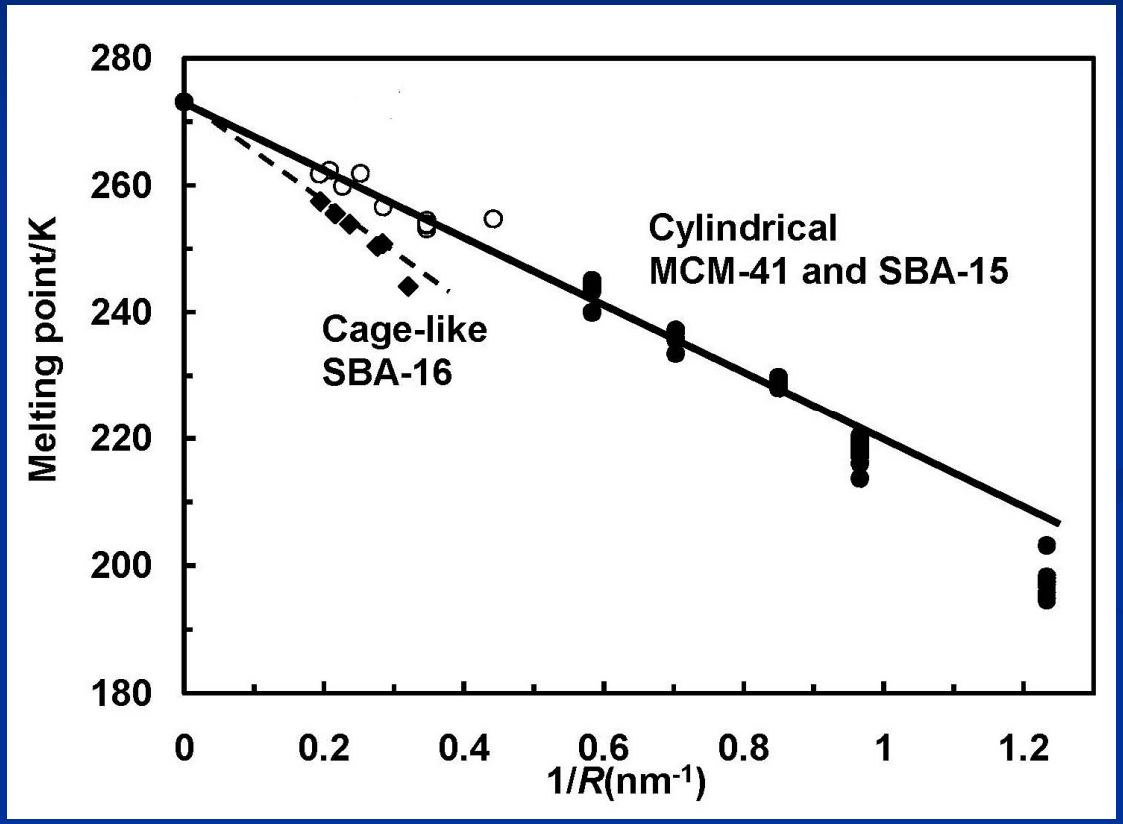

The Gibbs-Thomson relation tends to deviate from linearity above $1/R$ ~0.8 (pore size < ~3.3 nm).

$$\Delta T = \frac{2\nu\Delta\gamma_{l-s}}{\Delta H_m R_{cy}} T_0,$$

ν: Molar volume of water
$\Delta\nu_{l-s}$: Interfacial free energy change from wall/ice to wall/liquid
ΔH_m: Enthalpy change in melting of ice
R_{cy} : Effective pore size
T_0 : Melting point of bulk water

Effective pore size $R = a - t$
a: intrinsic pore radius
t: thickness of unfrozen layer of water at the interface (0.38 nm)

FTIR spectra of the O-H stretching band of bulk water (left) and water confined in MCM-41 C10 (right) on JEOL JIR-100

Kittaka, Ishimaru, Kuranishi, Matsuda, TY, PCCP, 8 (2006) 3223.

$E = h\nu$ (ν: wavenumber)

O–H····O–

No significant shifts at 263 – 213 K in bulk ice

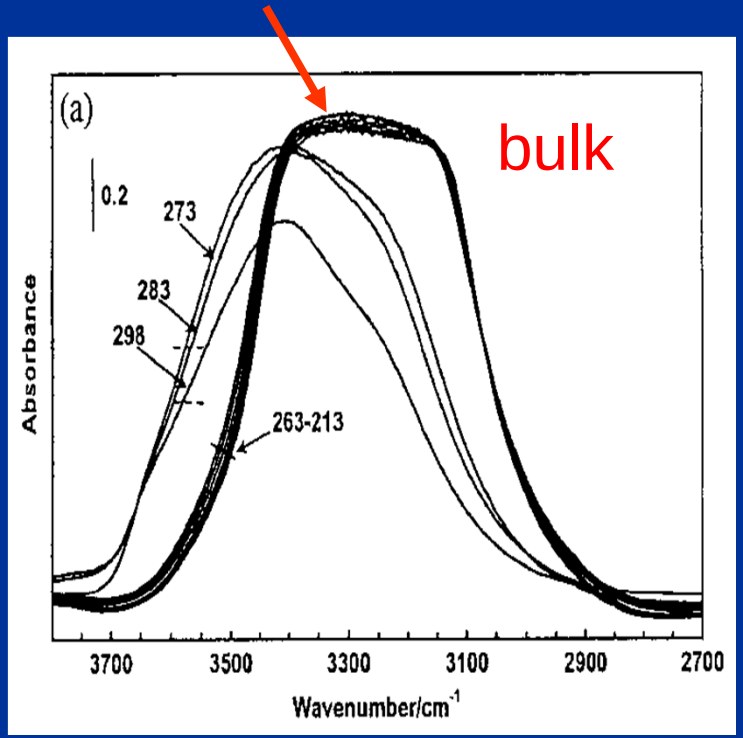

Continuous shift to the lower wavenumber with cooling to 173 K, suggesting strengthening H-bonds.

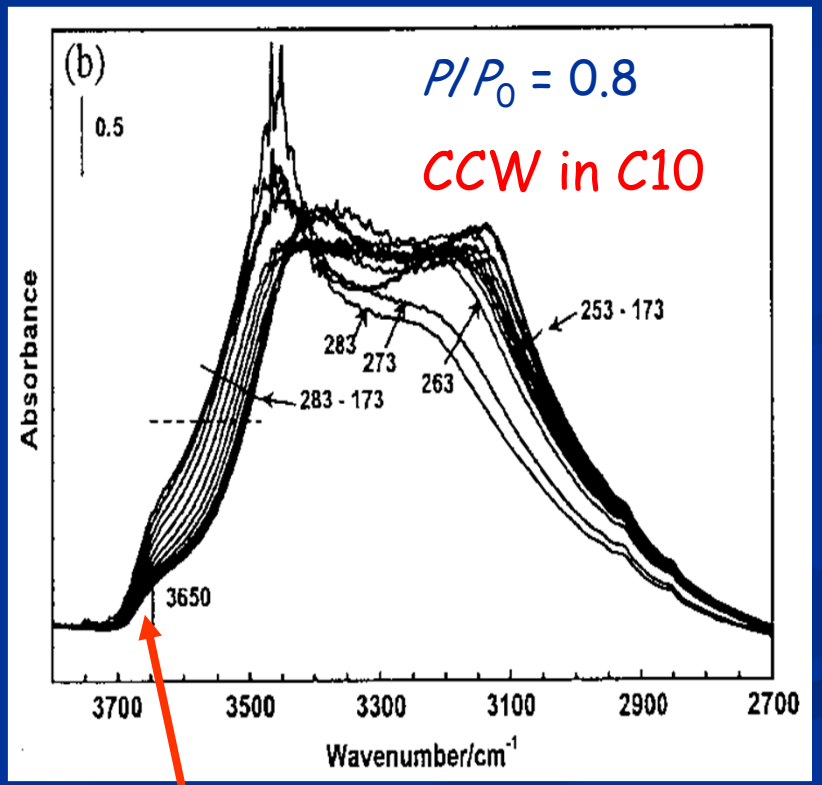

Surface hydroxyls at 3650 cm^{-1}

Frequency shift @Abs=1 of the O-H band of bulk water and water confined in various MCM-41s

Kittaka, Ishimaru, Kuranishi, Matsuda, TY, *PCCP*, 8 (2006) 3223.

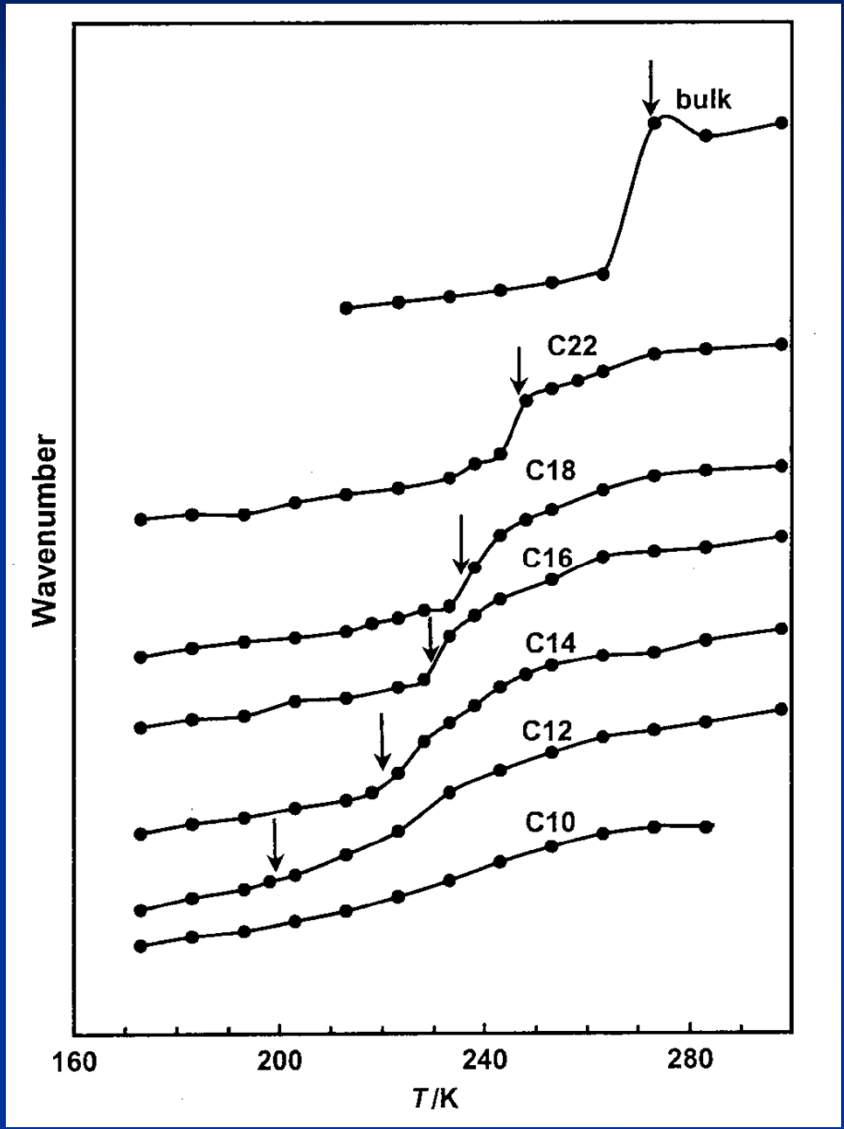

Arrows show the melting point of confined water, where the band edges shift remarkably to the lower wavenumber due to freezing.

For the MCM-41 with smaller pores, the band shits are less pronounced, reflecting the propensity of freezing of confined water.

Even in the case of C10 the band shift has an inflection point at ~230 K, indicating some transition of confined water.

How can we see the structure of water in silica pores by X-ray and neutron diffraction?

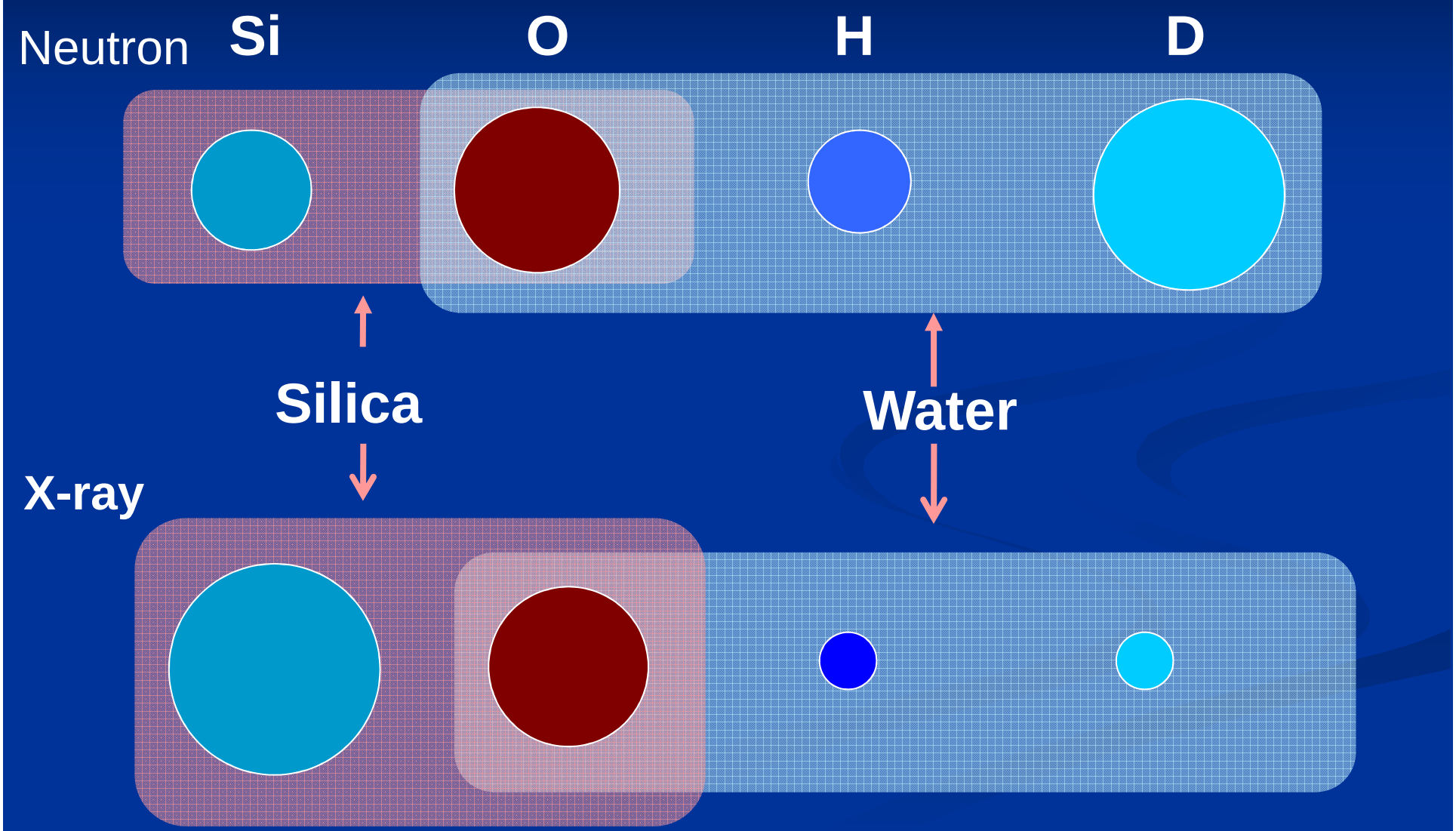

Fundamental terms used in X-ray and neutron scattering

Coherent scattering Elastic scattering	$\lambda_i = \lambda_s$	Structure (distance, coordination number)
Incoherent scattering Inelastic scattering	$\lambda_i \neq \lambda_s$	Dynamics(vibration, translation, rotation)

	X-ray	Neutron	
	Z(Atomic Number)	f ($x10^{-12}$cm)	σ_{inco}(barns)
H	1	–0.394	79.7
D	1	0.667	2.0
O	8	0.580	< 0.015
Si	14		

H_2O single particle dynamics, D_2O collective dynamics

Microscopic structure of water

Structure factors

$S(Q) = \sum\sum c_i c_j b_i b_j s_{ij}(Q)$ $s_{ij}(Q)$ psf of pair i-j

Radial distribution function

$g(r) = 1 + (1/\ 2\pi^2 \rho_0)\int Q(S(Q)-1)\sin(Qr)dQ$

- X-ray diffraction
- Neutron diffraction with H/D isotopic substitution
- Empirical potential structure refinement

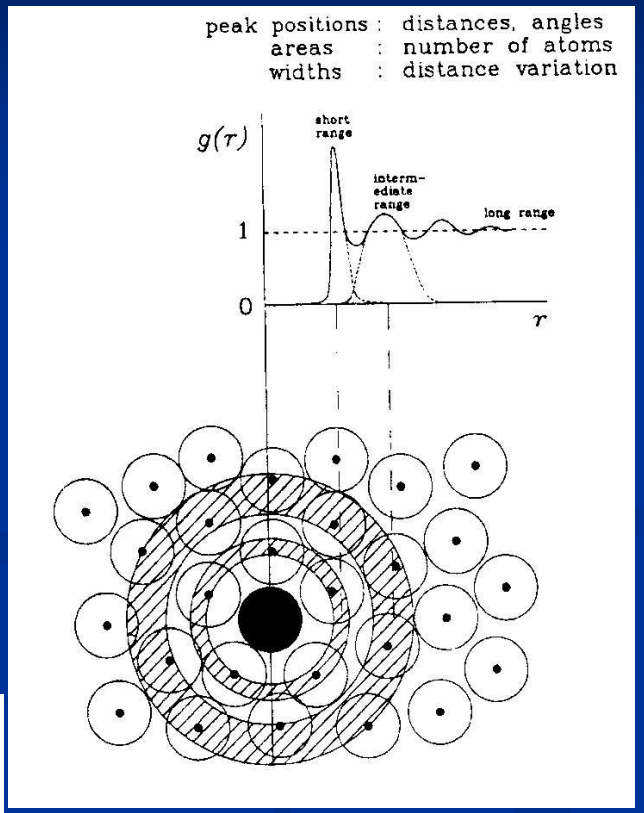

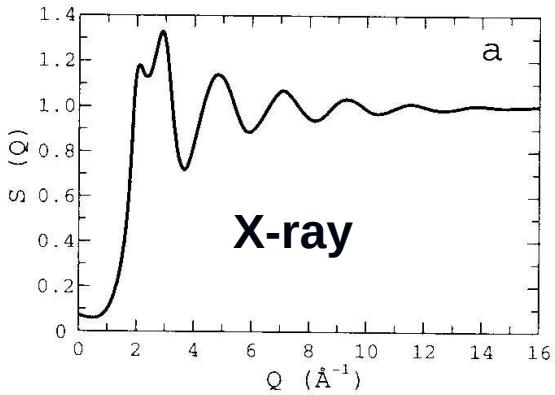

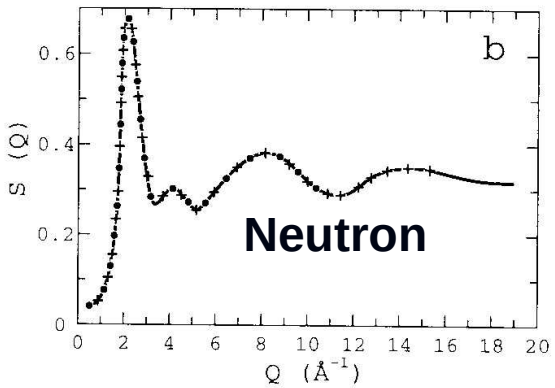

Empirical potential structure refinement

A.K. Soper, Chem Phys, 202 (1996) 296; Mol Phys, 99 (2001) 1503

1. Initiate simulation with any given site-site potential.
2. Calculate the potential of mean force by

$$\Psi = -kT \ln(g(r))$$

3. Calculate the potential of mean force from diffraction data.

$$\Delta\Psi = \Psi^{D} - \Psi = -kT \ln(g(r) / g^{D}(r))$$

4. Modify the potential as

$$U^{(n+1)} = U^{(n)} + \Delta\Psi$$

5. Run the simulation with the new potentials until equilibrium is established.

Pair distribution functions of water

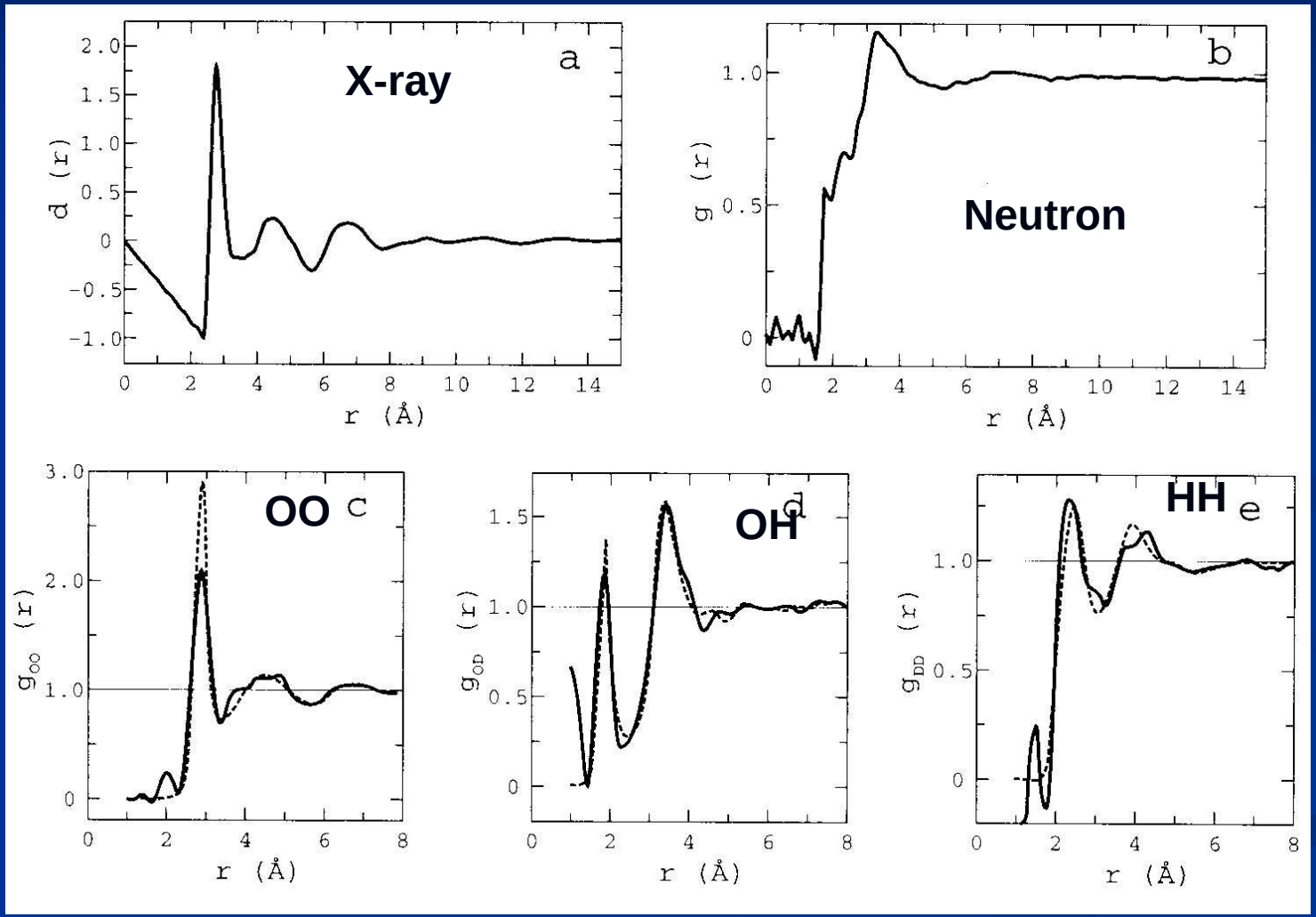

In-situ FTIR and XD with Imaging plate detector combined with a cryostat Mo Kα (λ=0.7107 A)

(Bruker AXS-DIP-301)

In situ FTIR

Vacuum & adsorption line

In situ XD with IP

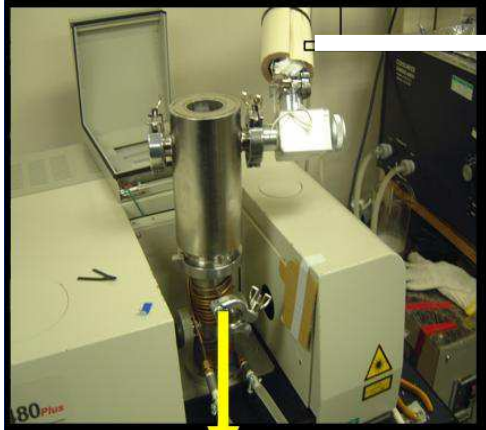

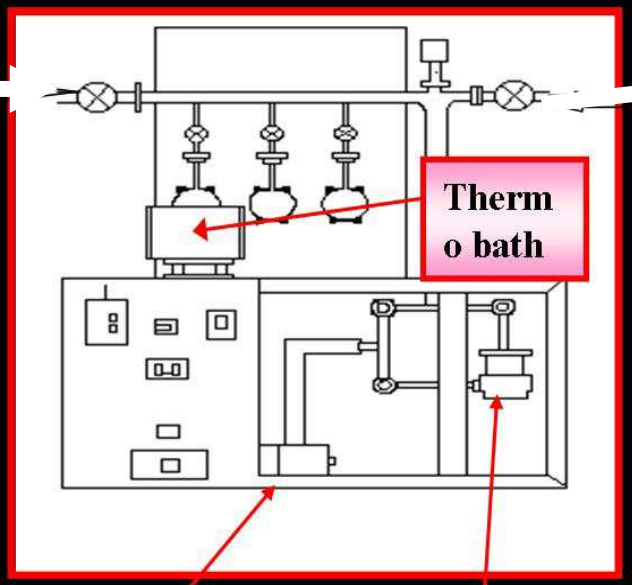

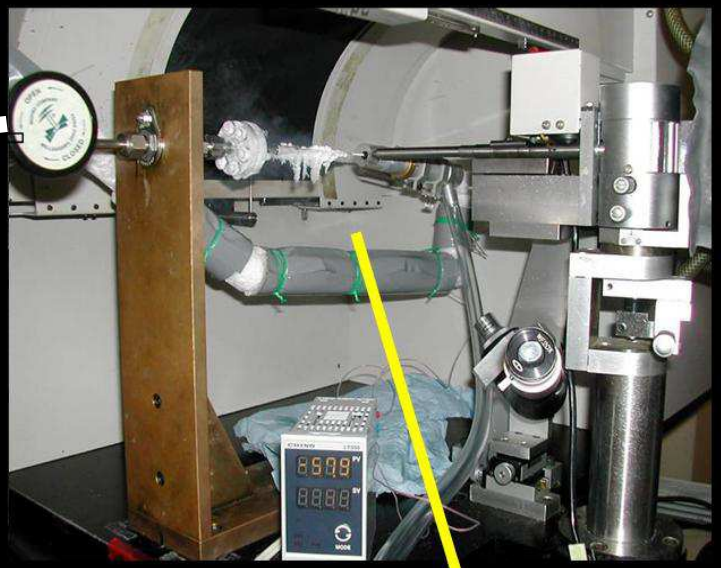

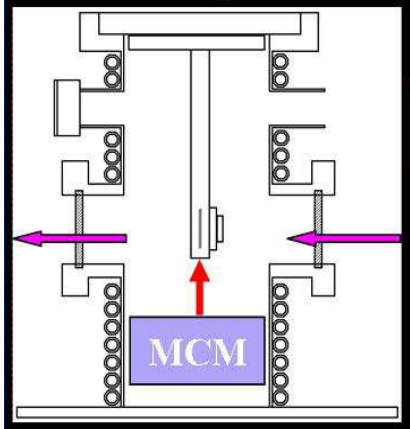

IR light

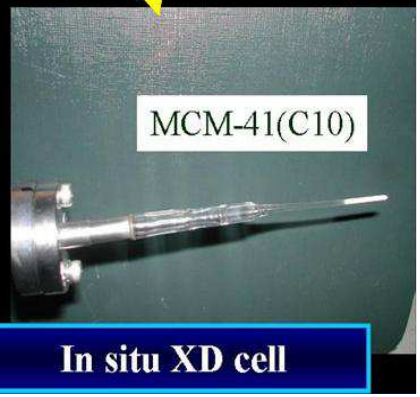

In situ XD cell

X-ray radial distribution functions of confined MLW and CCW in MCM-41 C14 (28 Å)

Smirnov, TY, Kittaka, Takahara, Kuroda, J. Phys. Chem. B, 104, 5498-5504 (2000).

CCW: Tetrahedral-like structure is distorted compare with bulk, and enhanced with lowering temperature

MLW: Tetrahedral-like structure is very distorted and practically independent of temperature

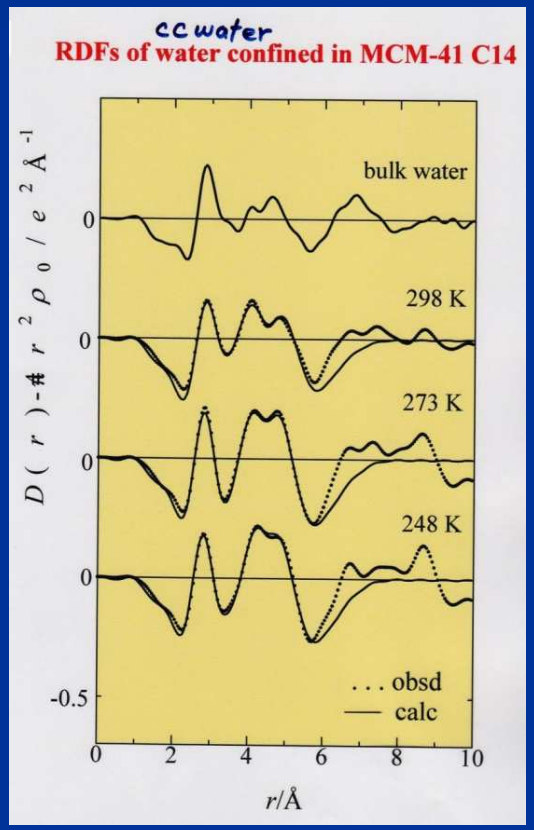

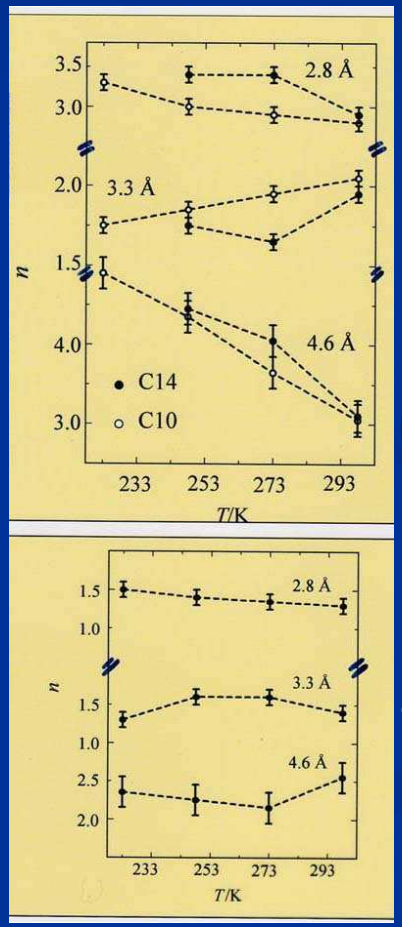

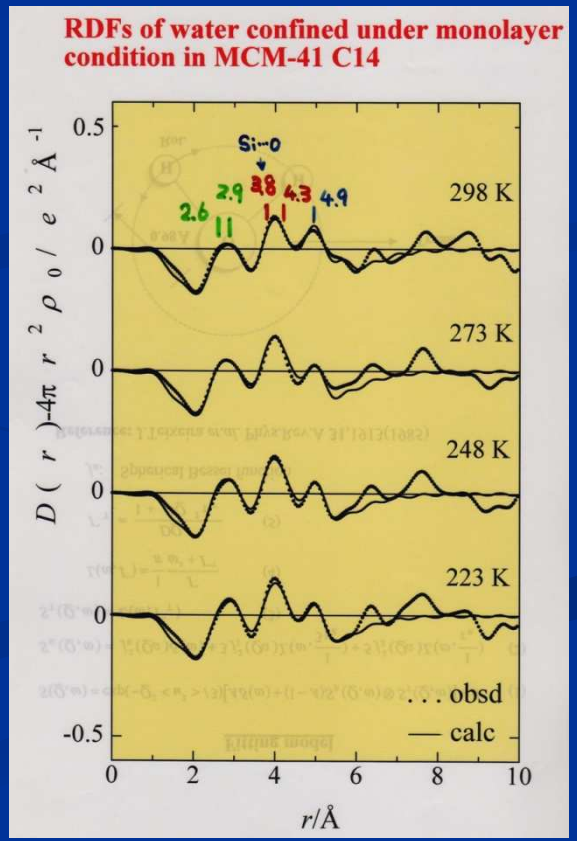

Summary on structure of water confined in MCM-41

The tetrahedral-like structure of confined water is distorted, compared with bulk, and it is more drastic for MLW due to the confinement and interfacial effects.

CCW in C10 pore (21 Å) showed structural transformation from HDA-like to LDA-like at 220-230 K, which is caused by water in the central part of the pore.

H-bonded network is reinforced for water in the central region of pore with lowering temperature.

The structure of MLW is practically independent of temperature.

Dynamic properties of liquid water

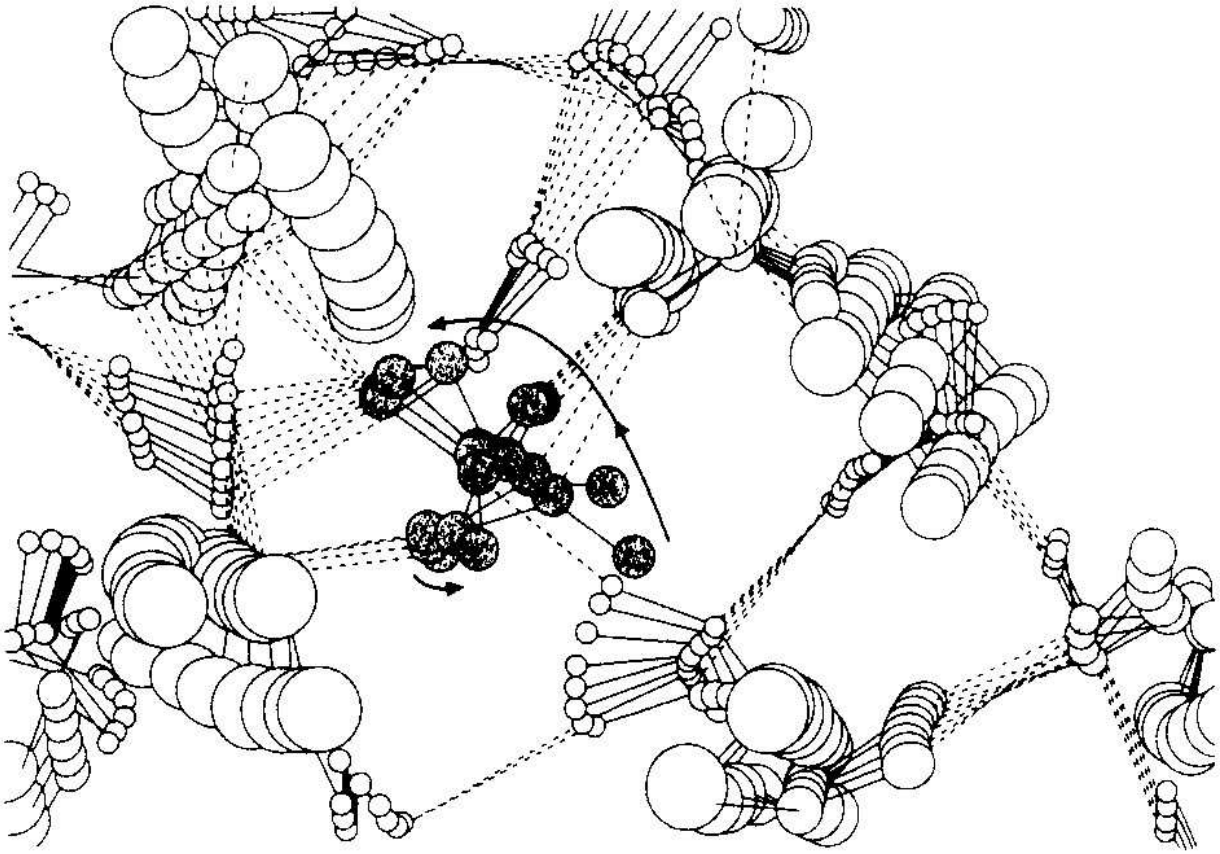

図 1　0.3 ps間のTIP2Pモデル水の動き[3)]

H. Tanaka, I. Ohmine, JCP, 87 (1987) 6128.

Quasielastic and inelastic scattering

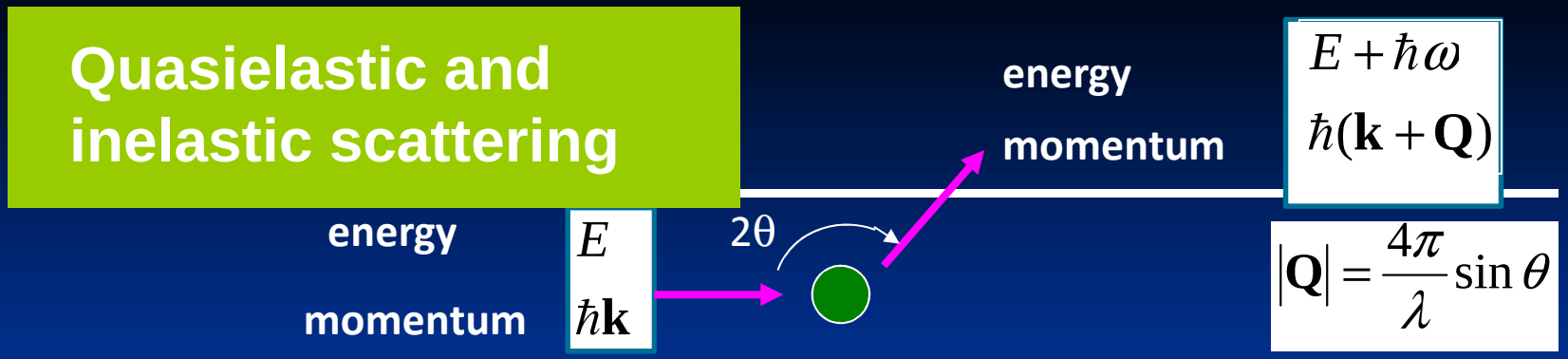

Energy and momentum transfers → **Information of structure and dynamics**

Intermediate scattering function

Neutron spin echo

$$I(Q,t) = N^{-1}\sum_{k,l}\left\langle \exp(i\mathbf{Q}\cdot\mathbf{r}_k(0))\cdot\exp(-i\mathbf{Q}\cdot\mathbf{r}_l(t))\right\rangle$$

$\mathbf{r}_k(0)$ position of atom of k at t= 0

$\mathbf{r}_l(t)$ position of atom of l at t

$k = l$ incoherent

$k = l$ coherent

$$S(Q,\omega) = \frac{1}{2\pi}\int_{-\infty}^{\infty} dt \int d\mathbf{r} g(\mathbf{r},t) e^{i(\mathbf{Q}\cdot\mathbf{r}-\omega t)}$$

Dynamical structure factor

van Hove's time-space correlation function

Inelastic neutron scattering techniques for dynamics properties at different length and time scales

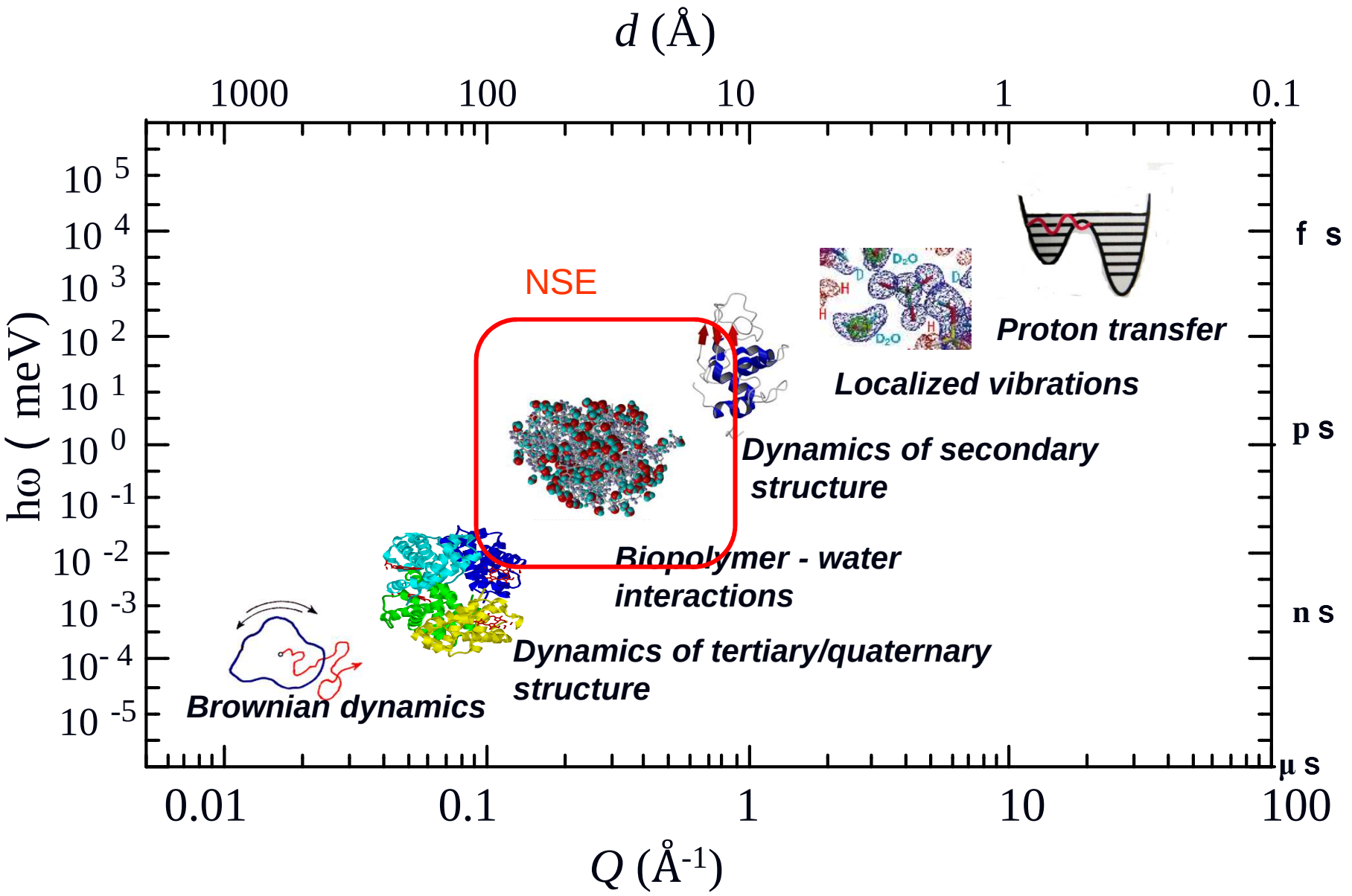

Dynamics Neutron spin echo technique measures inelastic scattering of water over energy *E* and length *Q* scale

Neutron spins

Incident neutrons lose energy due to inelastic process for the motion of water.

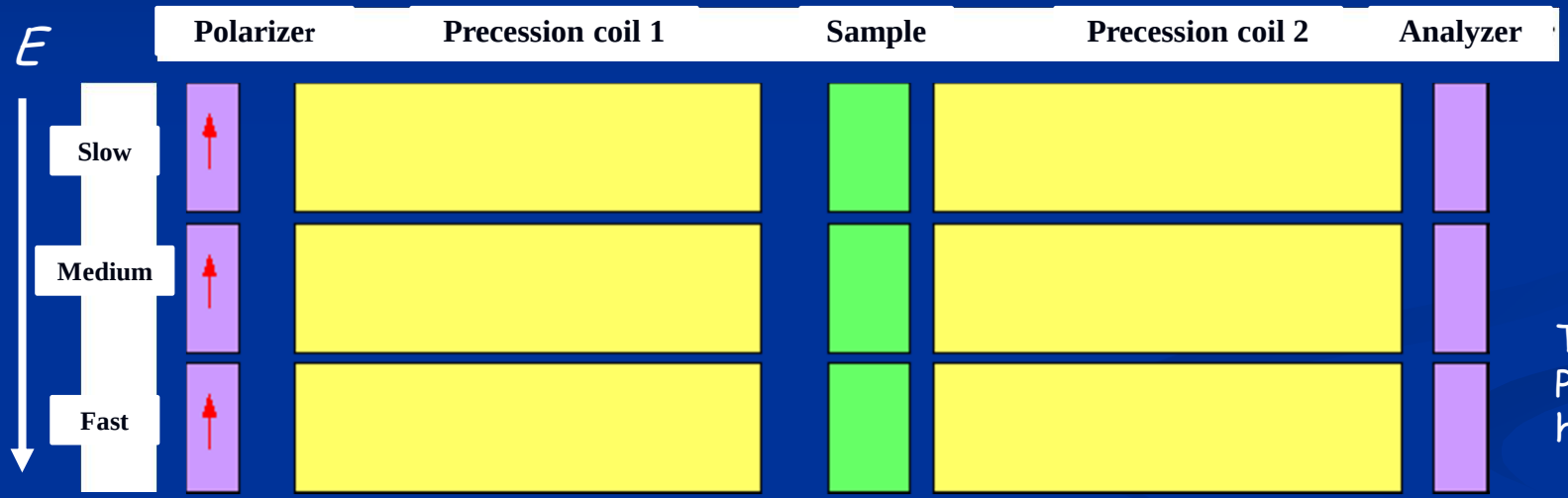

Taken from Prof. Seto's homepage

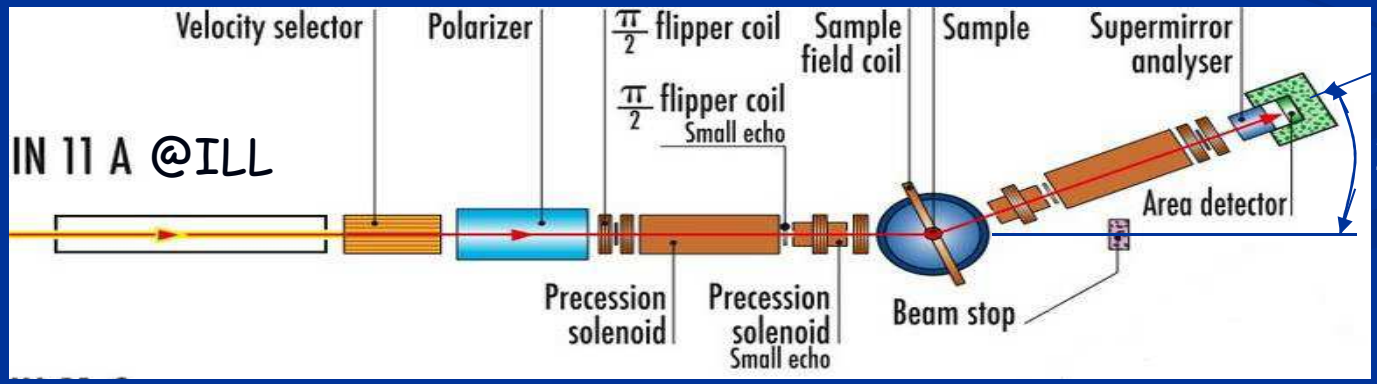

$Q = 4\pi \sin\theta/\lambda$

$= 2\pi/d$

Taken from ILL homepage

Intermediate scattering functions $I(Q,t)$ of CC D_2O confined in MCM-41 C10 obtained by NSE

Yoshida, TY, Kittaka, Bellissent-Funel, Fouquet, JCP, 129 (2008) 54702.

Q = 17 nm^{-1}

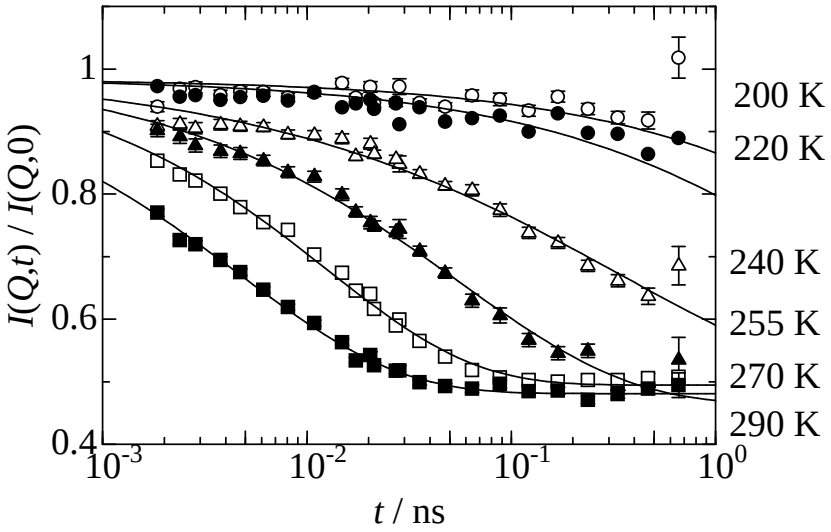

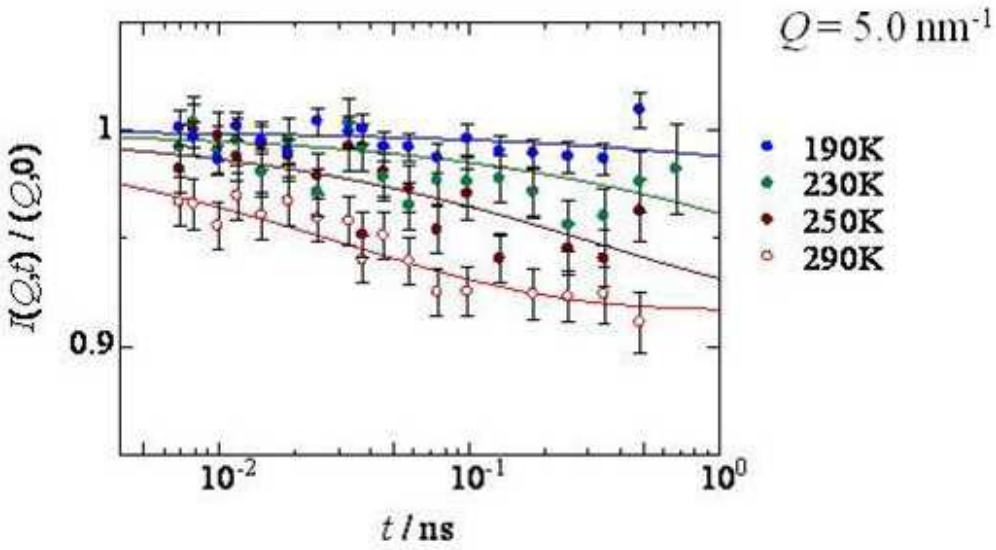

Kohlrausch-Williams-Watts (KWW) stretched exponential function

$$I(Q,t) = (1-p(Q))A(Q)\exp\left\{-\left(\frac{t}{\tau(Q)}\right)^{\beta(Q)}\right\} + p(Q)$$

$A(Q)$ Debye-Waller factor
$\tau(Q)$ relaxation time
$b(Q)$ stretched exponent
$p(Q)$ elastic term attributed to silica

Dynamic properties of water confined in MCM-41 C10

K. Yoshida, T.Y., S. Kittaka, M.-C. Bellissent-Funel, P. Fouquet, J. Phys.: Condens. Matter, 24, 064101 (2012)

Vogel-Fulcher-Tamman (VFT) equation

$$\tau(Q) = \tau_0(Q)\exp\left(\frac{D(Q)T_0(Q)}{T - T_0(Q)}\right)$$

$\tau_0(Q)$ pre-exponential factor
$D(Q)$ fragility
$T_0(Q)$ ideal glass transition temperature

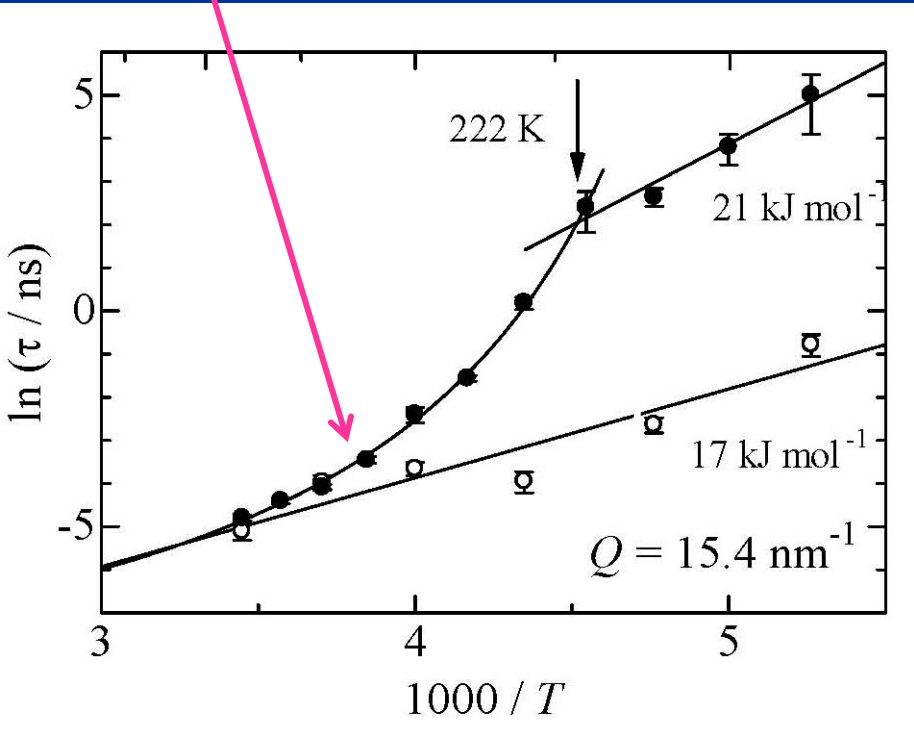

Monolayer water
Arrhenius type behaviour
<Ea> = 17 kJ/mol

Capillary condensed water
T>~220 K VFT behaviour
Fragile liquid
high density liquid
T<~220 K Arrhenius type
Strong liquid
low density liquid
<Ea> = 21 kJ/mol

Fragile To Strong (FTS) dynamical crossover arises from water in the central region of the pore.

Outline

- Introduction *Why is confined water important?*
- Water in MCM-41
- Water in periodic mesoporous organosilica
- Conclusions and Perspectives

Periodic Mesoporous Organosilica (PMO)

Inagaki, Nature, 416 (2002) 304

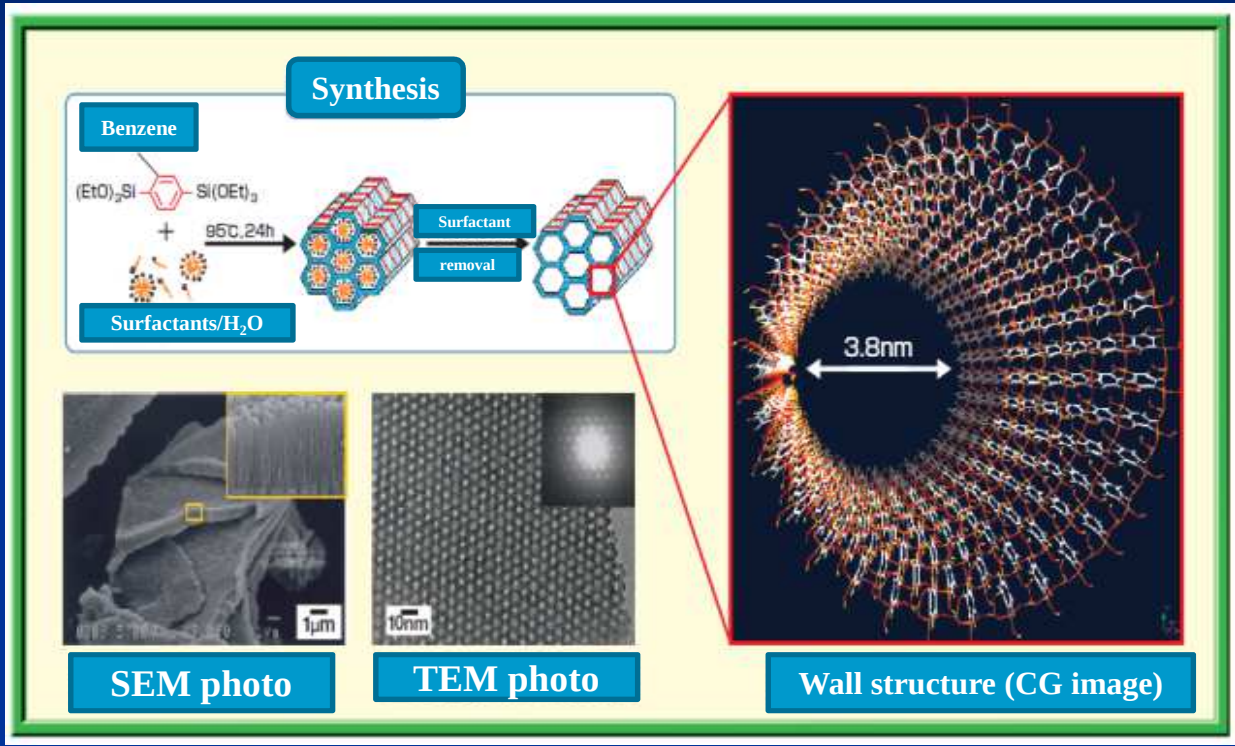

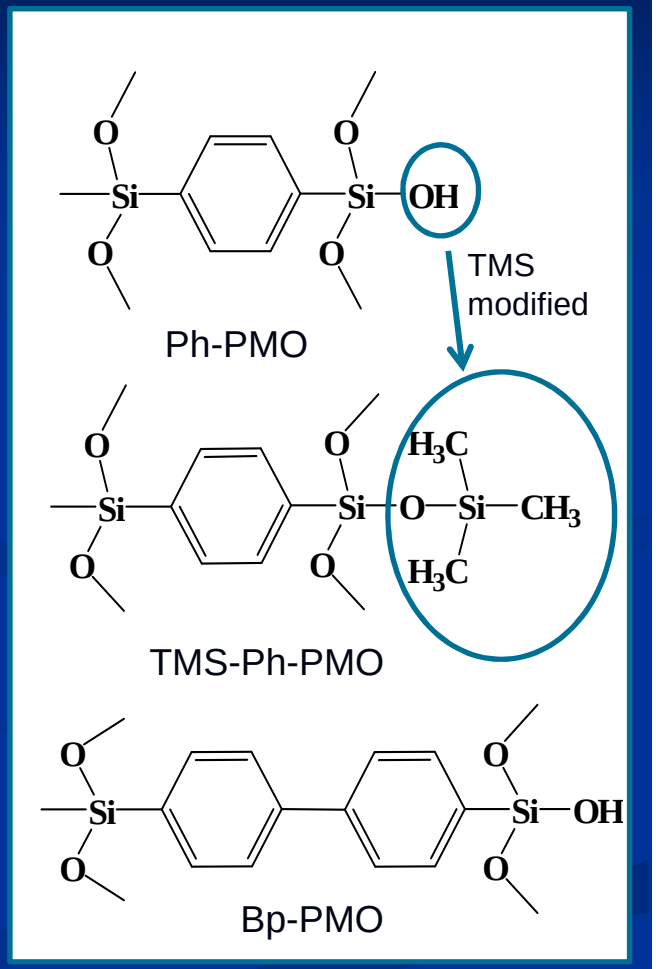

Organic groups are embedded in silica matrix to generate inorganic-organic hybrid surface, which allows us to tune the balance between the hydrophilic and hydrophobic nature of the wall.

Various PMOs so far prepared

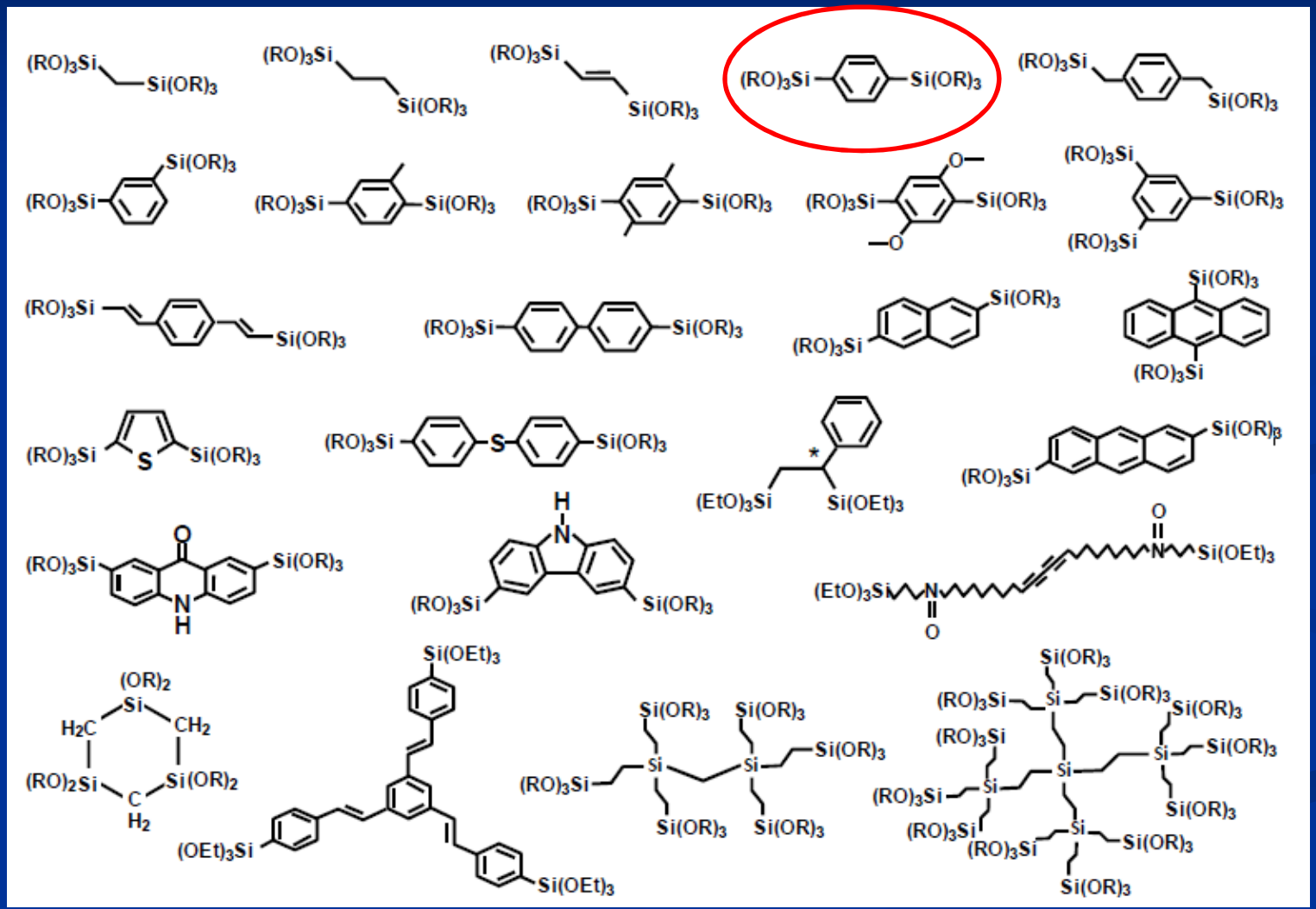

Periodic Mesoporous Organosilica (PMO): organic-inorganic hybrid surface capable of tuning the balance between hydrophobic and hydrophilic nature of pore wall

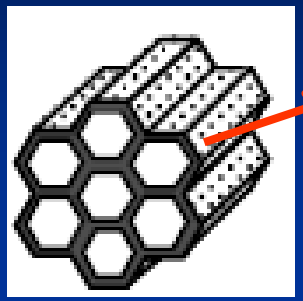

S. Inagaki (Toyota Central Laboratory)

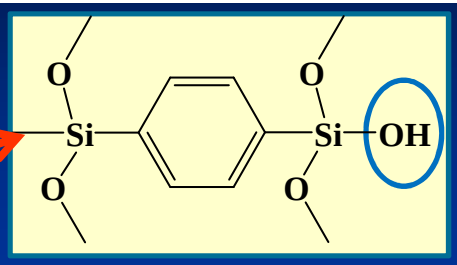

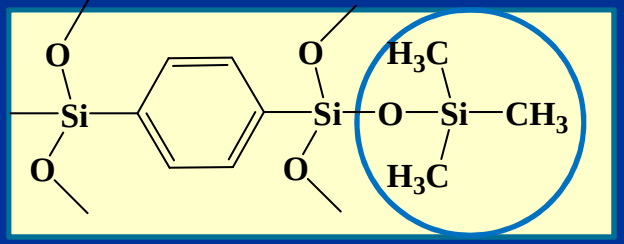

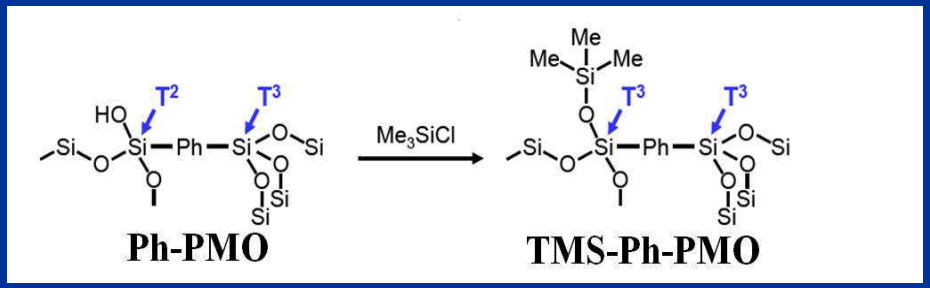

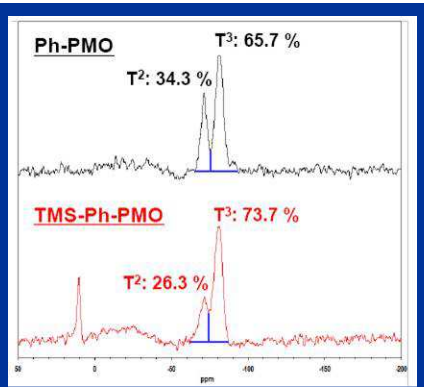

^{29}Si NMR spectra showed the OH sites were modified only by 8% with TMS

N_2 adsorption

Ph-PMO
- d_p 27.18Å
- V_p 1.00 cm^3/g
- S_p 2309 m^2/g

TMS-Ph-PMO
- d_p 27.14Å
- V_p 1.04 cm^3/g
- S_p 2089 m^2/g

cf. MCM-41 C14
- d_p 28.4Å
- V_p 0.93 cm^3/g
- S_p 1300 m^2/g

Water adsorption /desorption isotherms

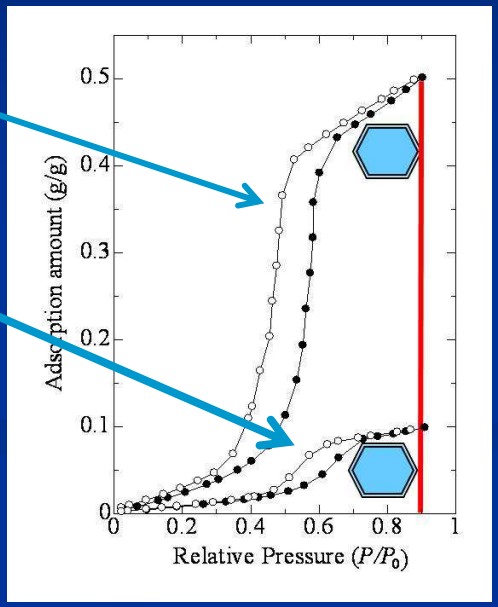

It should be noted that hydrophobic modification only by 8% drastically decreased the adsorption amount of water.

DSC and XRD data on low-temperature water confined in Ph-PMO

Aso, Ito, Sugino, Yoshida, Yamada, Yamamuro, Inagaki, T.Y. Pure Appl. Chem. In press.

DSC data (MCM-41 C14 data)

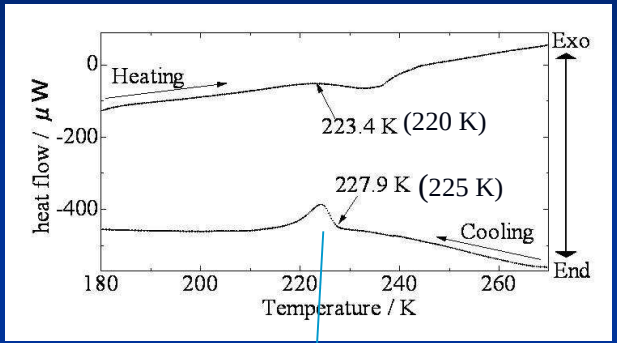

XRD data

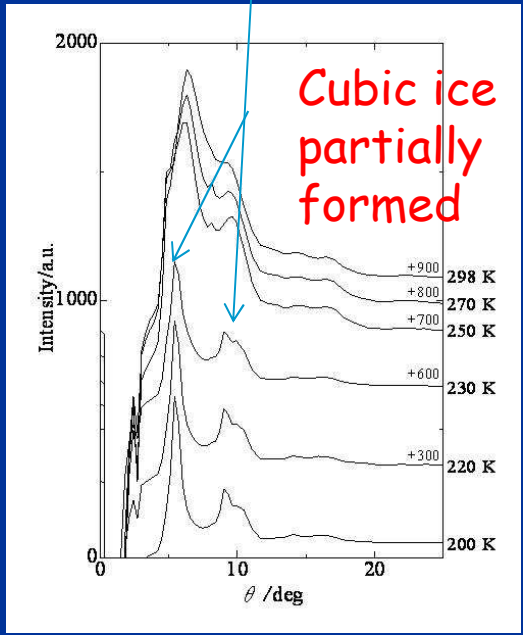

X-ray radial distribution functions

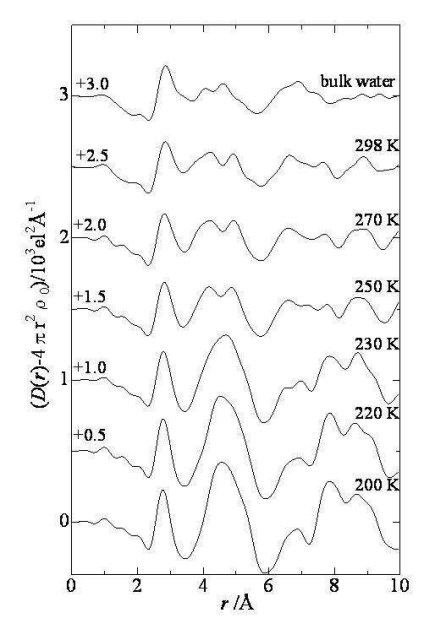

Coordination number vs. T

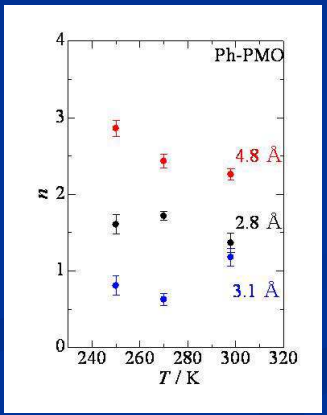

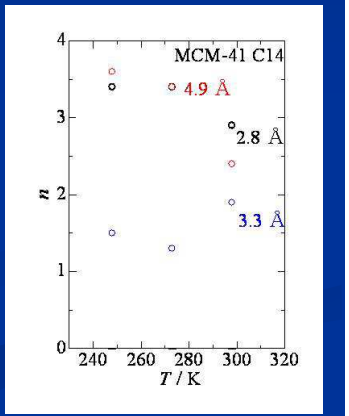

RDF features show that H-bonded structure is more distorted in Ph-PMO than in bulk.
With a decrease in temperature, the H-bonded structure tends to recover a tetrahedral geometry, evidenced by lowering CN of 3.1 Å peak (non-H-bond) and increasing CNs of 2.8 and 4.8 Å (H-bond).

Quasi-Elastic Neutron Scattering, QENS)

on AGNES(Angle-focusing Neutron Spectrometer) @JRR-3, Tokai, Japan.

Overview of AGNES

Schematic of data on AGNES

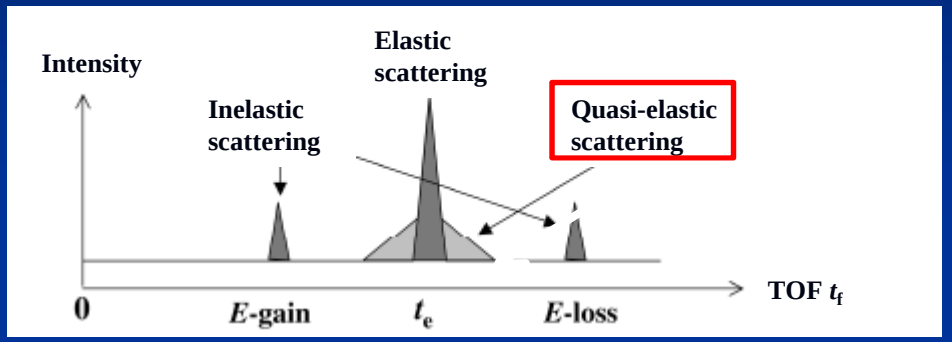

Elastic scattering →structure
Inelastic scattering →vibration
Quasi-elastic →diffusion

Spectrometer

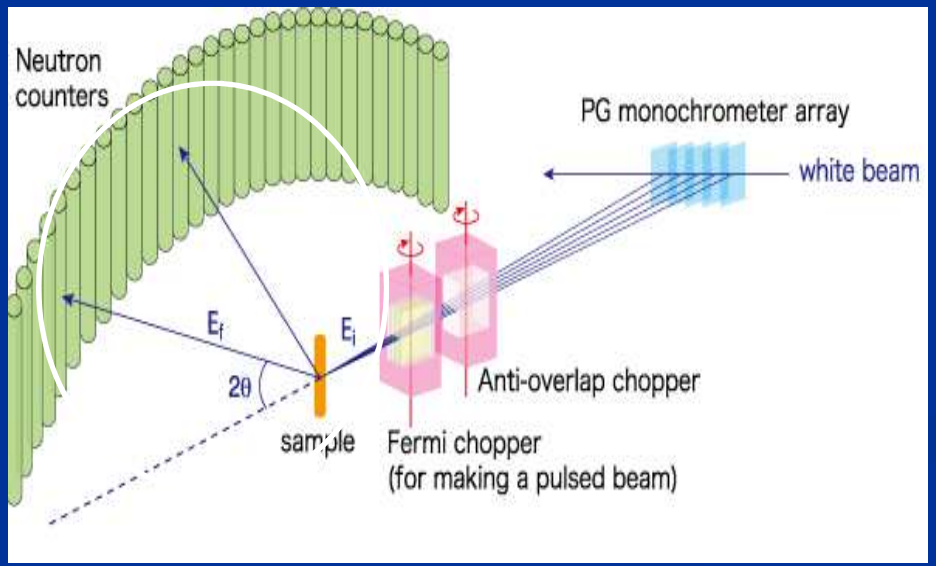

Scattered neutrons

Incident neutrons

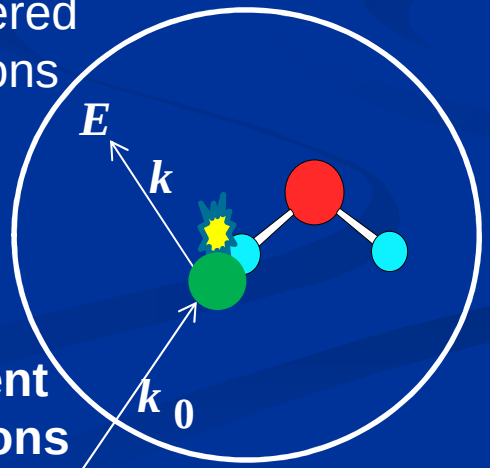

$h\omega = E - E_0$

$Q = k - k_0$

QENS spectra of water confined in Ph-PMO @Q = 1.6 Å^{-1} analyzed by a jump diffusion model

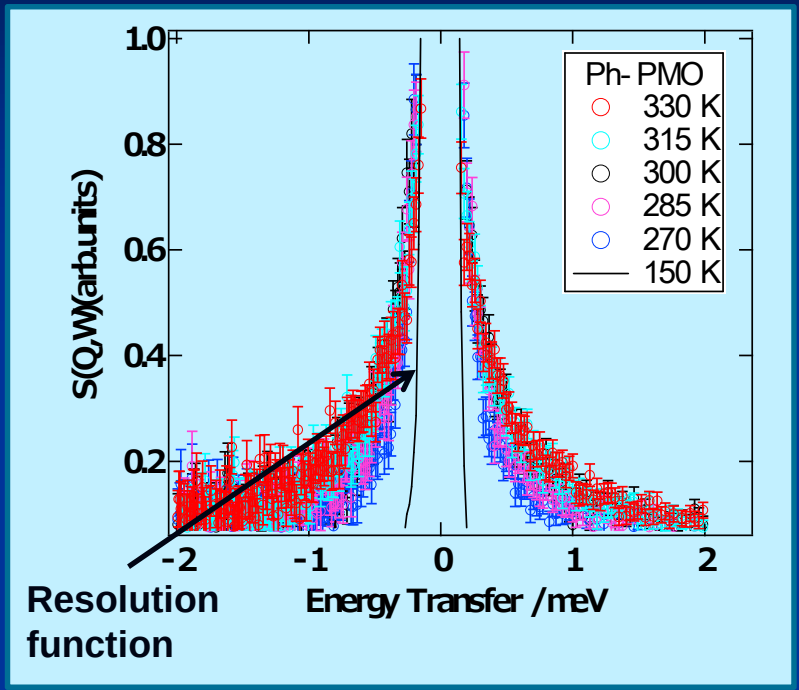

fitting

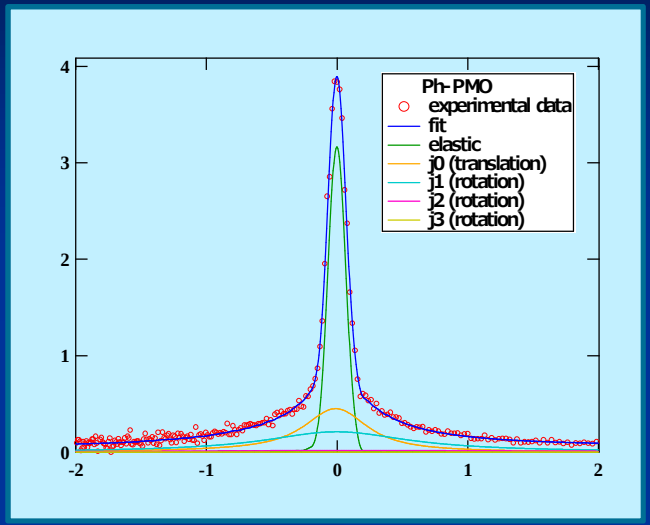

$$S(Q,\omega)=\left\{\delta(\omega)+\exp\left(-\frac{Q^2\langle u\rangle}{3}^2\right)L_{\mathrm{Trans}}(Q,\omega)\otimes L_{\mathrm{Rot}}(Q,\omega)\right\}\otimes R(Q,\omega)+BG$$

Translational motion

$$L_{\mathrm{Trans}}(Q,\omega)=\frac{1}{\pi}\left[\frac{\Gamma(Q)}{\omega^2+\Gamma(Q)^2}\right]$$

Rotational motion

$$L_{\mathrm{Rot}}(Q,\omega)=j_0^2(Qa)\delta(\omega)+\frac{1}{\pi}\sum_{l=1}^{\infty}(2l+1)\,j_l^2(Qa)\,\frac{l(l+1)D_{\mathrm{rot}}}{\omega^2+\left[l(l+1)D_{\mathrm{rot}}\right]^2}$$

Half-width at half maximum

$$\Gamma(Q)=\frac{DQ^2}{1+DQ^2\tau_0}$$

relaxation time

$$\tau_1=\frac{1}{6D_{\mathrm{rot}}}$$

Arrhenius plots of diffusion coefficient *D* for water in various mesoporous materials

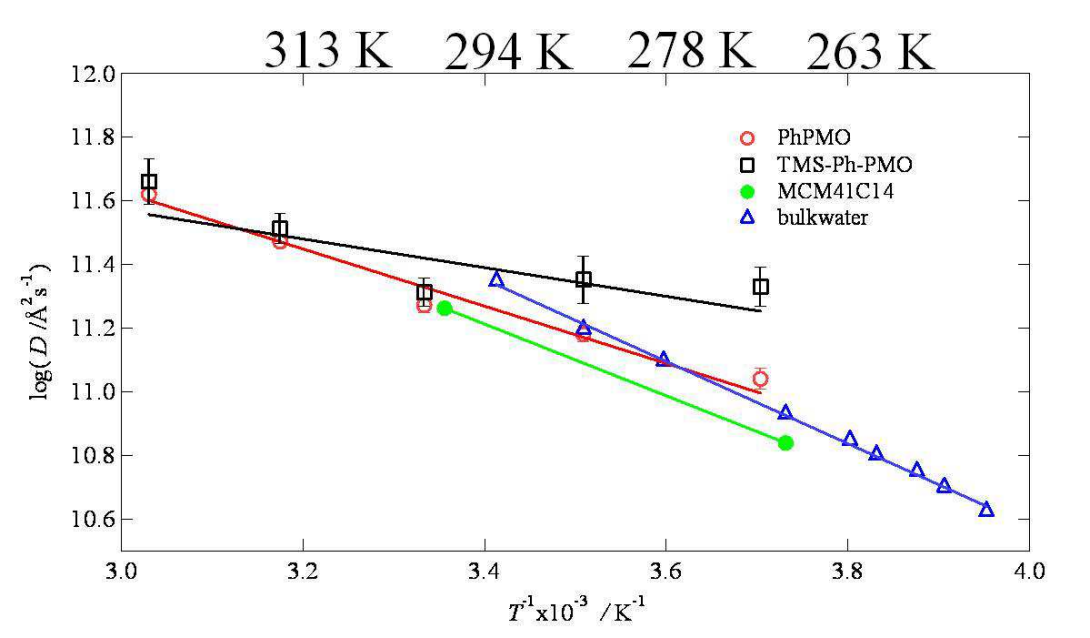

Activation energy E_a (kJ/mol) of translational motion

Modified ⟷ non-modified

TMS-Ph-PMO	Ph-PMO	MCM-41 C14	Bulk water
8.64 ± 2.28	17.2 ± 0.9	21.6[a]	17.9 ± 0.9 [b]

[a] S. Takahara, et al. *J. Phys. Chem. B*, 103. 5814 (1999).
[b] T. Yamada, et al. *J. Phys. Chem. B*, 115, 13563 (2011).

Confined water diffuses with a smaller energy than in bulk.
-> Effects of confinement and interfacial interaction.

With increasing hydrophobic nature of pore walls, confined water diffuses with a smaller activation energy.
-> Water molecules might assemble in the center of hydrophobic pores.

Arrhenius plots of rotational relaxation time τ for water in various mesoporous materials

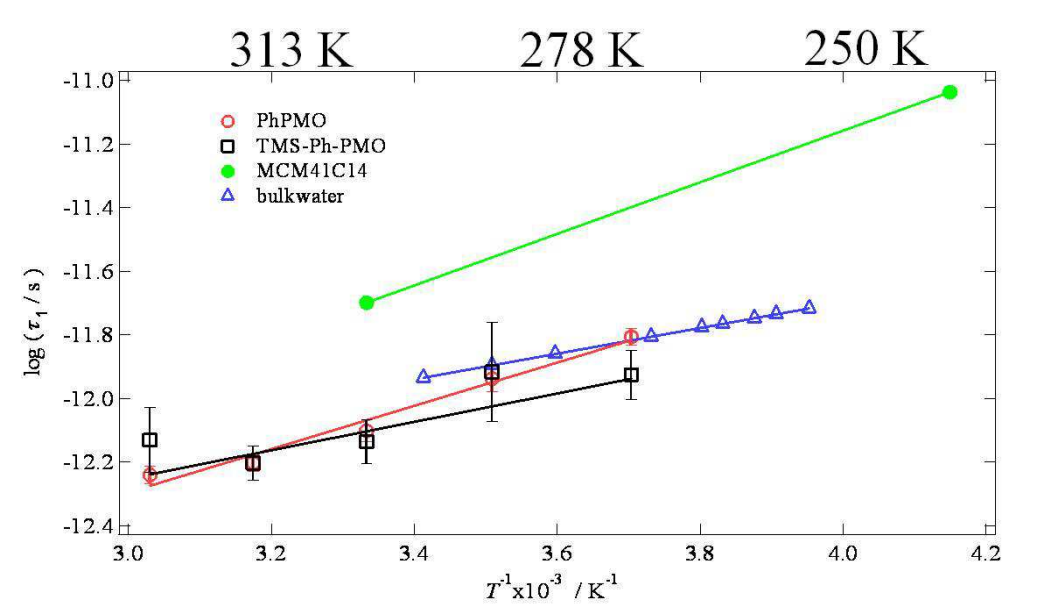

Activation energy E_a (kJ/mol) of rotational motion

Modified ⟷ non-modified

TMS-Ph-PMO	Ph-PMO	MCM-41 C14	Bulk water
8.55 ± 2.97	13.0 ± 1.0	15.6[a]	**13.5±0.8**[b]

[a] S. Takahara, et al. *J. Phys. Chem. B*, 103. 5814 (1999).
[b] T. Yamada, et al. *J. Phys. Chem. B*, 115, 13563 (2011).

Confined water rotates with a larger activation energy than in bulk.
-> Interaction with pore walls

When the hydrophobicity of pore walls decreases, confined water rotates with a larger activation energy.
-> Water molecules strongly interacts with the hydrophilic pore walls.

Conclusions and perspectives

- Structure and dynamics of liquids and solutions are affected by confinement (pore size) and interaction wit the surface (hydrophilicity-hydrophobicity), which reflects various functions of confined liquids and solutions.
- Synthesis of new porous materials – modification of the surface property, metal-organic-framework (MOF)
- Ionic liquids in confinement – green chemisry
- Biomolecules, such as enzymes, in confinement – to stabilize enzymes against denaturation agents, T, P
- Nanotechnology - chemical reactions in confinement – nanowire, nanodevice
- Medical applications - drug delivery system

Microscopic and mesoscopic range order diffractometer: NIMROD (ISIS) NOVA(J-PARC)

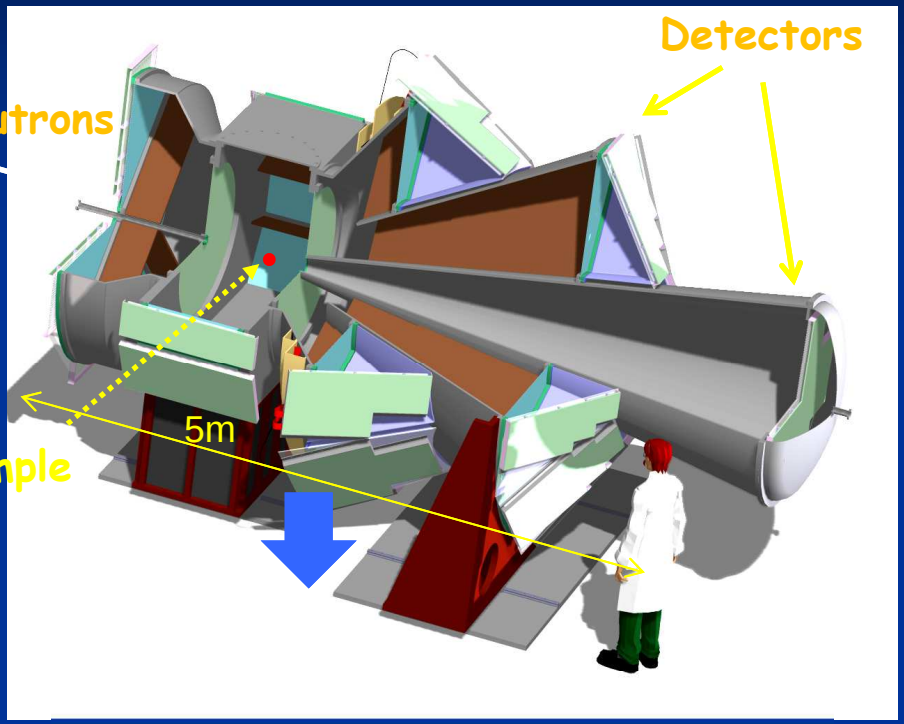

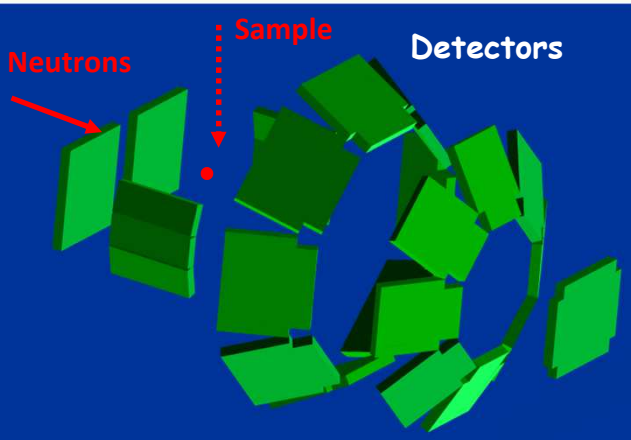

Q-range: 0.02 – 100 Å^{-1} 1~300 Å

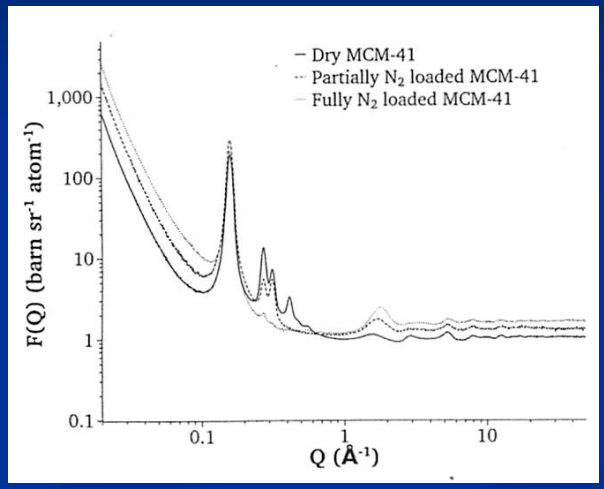

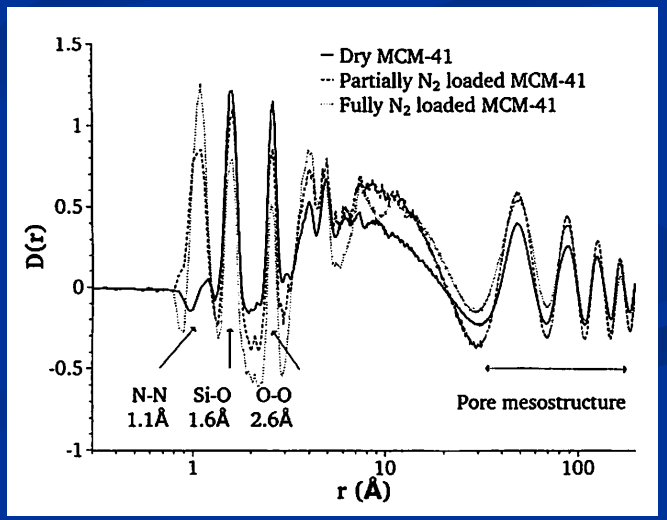

Bowron, Soper, Neutron News 22 (2011) 12

BL02 DNA: Dynamics Spectrometer

DNA is a High Energy Resolution Near-Backscattering Spectrometer

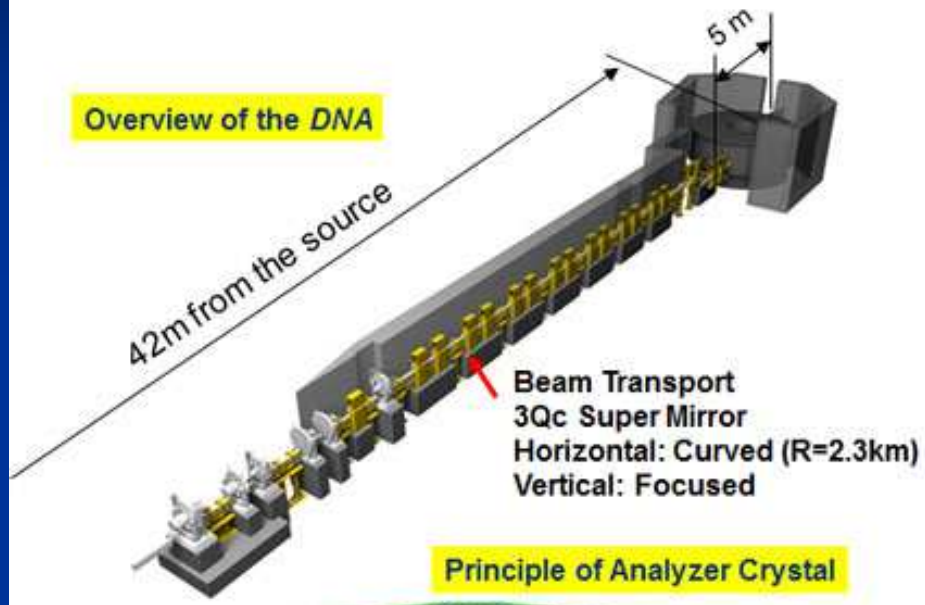

Source: Liq.H_2 Coupled Moderator (BL02)
Moderator-Sample:L_1 = 42 m
Sample-Detector: L_2 = 4.3 m,
Pulse-shaping device: L_{ch} = 7.75 m
Analyzer Bank: Spherical (R=2.3m)
Si(111)&Si(311)@θ_B=87.5 [deg.]
Si(111):δE = 1.2 μeV, Q_{max} = 1.9 Å^{-1}@elastic
Si(311):δE = 5 μeV, Q_{max} = 3.8 Å^{-1}@elastic
Horizontal Scat. Ang.:-164. < $2\theta_S$ < +164.[deg]
Vertical Scat. Ang.: -14. < $2\theta_S$ < +20.[deg]
High efficiency by RRM

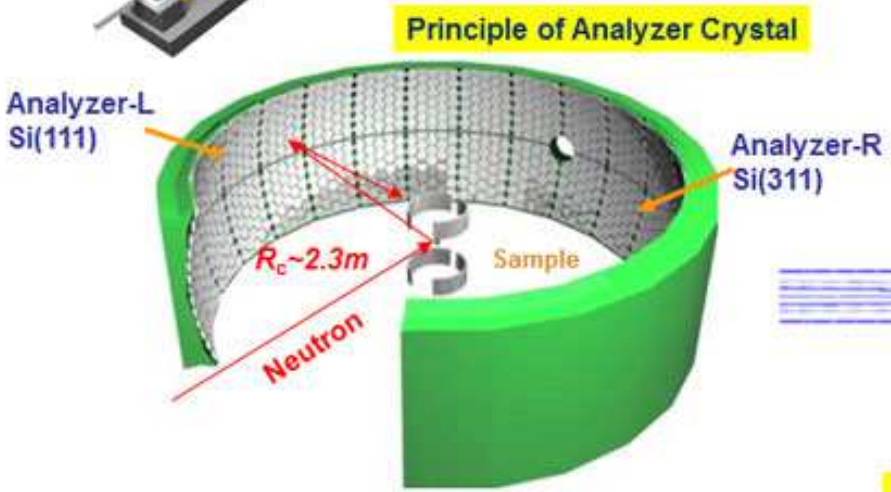

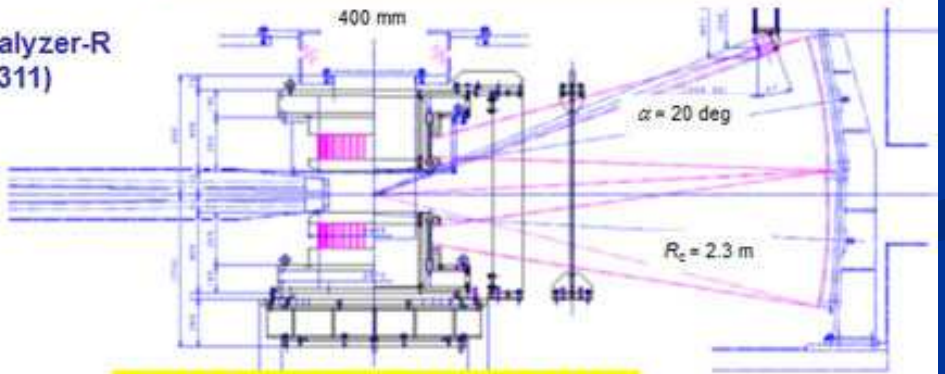

Section view of the scattering vessel

Acknowledgements

Prof. H. Wakita (Fukuoka U.)
Dr. K. Yoshida (Fukuoka U.)
K. Ito (Fukuoka U.)
M. Taguchi (Fukuoka U.)
T. Nagaki (Fukuoka U.)
K. Sugino (Fukuoka U.)
M. Aso (Fukuoka U.)
Prof. T. Takamuku (Saga U.)
Prof. S. Kittaka (Okayama Sci. U.)
Prof. S. Takahara (Okayama Sci. U.)
Prof. O. Yamamuro (U. Tokyo)
Dr. T. Yamada (CROSS Tokai)
Prof. Y. Miyake (Kansai U.)
Dr. S. Tanaka (Kansai U.)
Dr. S. Inagaki (Toyota Central Lab.)

Dr. P. Smirnov (Ivanovo, Russia)
Dr. A. K. Soper (ISIS, UK)
Dr. D. Bowron (ISIS, UK)
Dr. M. C. Bellissent-Funel (LLB, Saclay)
Dr. P. Fouquet (ILL, Grenoble)

Supported by MEXT & Fukuoka U.

Thank you for your kind attention

Bird-eye view of Fukuoka University